Received: 9 October 2024 | Accepted: 1 December 2024

DOI: 10.1111/jpy.13539

RESEARCH ARTICLE

Seasonality and interannual stability in the population genetic structure of *Batrachospermum gelatinosum* (Rhodophyta)

Sarah Shainker-Connelly[1] | **Solenn Stoeckel**[2] | **Morgan L. Vis**[3] | **Roseanna M. Crowell**[3] | **Stacy A. Krueger-Hadfield**[1,4]

[1]Department of Biology, University of Alabama at Birmingham, Birmingham, Alabama, USA

[2]DECOD (Ecosystem Dynamics and Sustainability), INRAE, Institut Agro, IFREMER, Rennes, France

[3]Department of Environmental and Plant Biology, Ohio University, Athens, Ohio, USA

[4]Virginia Institute of Marine Science Eastern Shore Laboratory, Wachapreague, Virginia, USA

Correspondence
Stacy A. Krueger-Hadfield, Virginia Institute of Marine Science Eastern Shore Laboratory, Wachapreague, VA 23480, USA.
Email: sakh@vims.edu

Funding information
Ohio University Student Enhancement Award; Agence Nationale de la Recherche, Grant/Award Number: Clonix2D ANR-18-CE32-0001; College of Arts and Sciences at UAB, Grant/Award Number: Start up funds; National Science Foundation, Grant/Award Number: Career Award DEB-2141971; UAB Blazer Fellowship; National Science Foundation, Grant/Award Number: EAGER DEB-2113745; Norma J. Lang Early Career Fellowship from the Phycological Society of America; Ohio Center for Ecology and Evolutionary Studies Fellowship; Ohio University Roach Fund; Ohio University Graduate Student Senate Original Work Grant; UAB Department of Biology's Harold Martin Outstanding Student Development Award

Editor: M. Roleda

Abstract

Temporal population genetic studies have investigated evolutionary processes, but few have characterized reproductive system variation. Yet, temporal sampling may improve our understanding of reproductive system evolution through the assessment of the relative rates of selfing, outcrossing, and clonality. In this study, we focused on the monoicous, haploid-diploid freshwater red alga *Batrachospermum gelatinosum*. This species has a perennial, microscopic diploid phase (chantransia) that produces an ephemeral, macroscopic haploid phase (gametophyte). Recent work focusing on single-time point genotyping suggested high rates of intragametophytic selfing, although there was variation among sites. We expand on this work by genotyping 191 gametophytes sampled from four sites that had reproductive system variation based on single-snapshot genotyping. For this study, we sampled at multiple time points within and among years. Results from intra-annual data suggested shifts in gametophytic genotypes throughout the season. We hypothesize that this pattern is likely due to the seasonality of the life cycle and the timing of meiosis among the chantransia. Interannual patterns were characterized by consistent genotypic and genetic composition, indicating stability in the prevailing reproductive system through time. Yet, our study identified limits by which available theoretical predictions and analytical tools can resolve reproductive system variation using haploid data. There is a need to develop new analytical tools to understand the evolution of sex by expanding our ability to characterize the spatiotemporal variation in reproductive systems across diverse life cycles.

KEYWORDS
algae, ploidy, reproduction, sex, stream, temporal patterns

Abbreviations: BSA, bovine serum albumen; DNA, deoxyribonucleic acid; dNTP, deoxynucleoside triphosphate; GPS, Global Positioning System; MLG, multilocus genotype; PCR, polymerase chain reaction.

INTRODUCTION

Traditionally, population genetic studies have aimed to characterize spatial genetic diversity and structure from samples collected at single time points from multiple sites (Storfer et al., 2007; Whitlock, 1992). Fewer studies have characterized temporal genetic diversity and structure by incorporating samples collected at multiple time points (Storfer et al., 2007; Whitlock, 1992). Yet, temporal genotyping has previously been used to address several types of ecological and evolutionary questions, including estimating population size (Waples, 1989), measuring evolutionary processes through time (Drummond et al., 2003), and assessing natural selection through time (e.g., from climate change, Jump et al., 2006; variable environmental conditions, Gómez et al., 1995; ecological succession, Linhart & Grant, 1996; or during biological invasions, Forsström et al., 2017). Although temporal variation likely also affects the prevailing reproductive mode, most studies assessing the reproductive system (i.e., the relative rates of sexual versus asexual reproduction and outcrossing versus selfing; Barrett, 2011) have only sampled a population once (e.g., Whitehead et al., 2018). Ecological variation, such as spatial and temporal fluctuation in pollinators (Barrett, 2015; Coates et al., 2013), can drive temporal variation in outcrossing rates within and among years (Whitehead et al., 2018), thereby influencing the partitioning of genetic diversity within and among populations. Additionally, in partially clonal organisms that can reproduce both sexually and asexually (often simultaneously), environmental conditions can result in different relative rates of sexual versus asexual reproduction through time (Bengtsson & Ceplitis, 2000; Gilabert et al., 2009; Liu et al., 2013; Weeks, 1993). For example, environmental stress can cause sexual reproduction in some aphid lineages (Simon et al., 2010), and seasonal changes can drive alternations of sexual and asexual reproduction in some microalgae (e.g., Dia et al., 2014; Lebret et al., 2012). Halkett et al. (2005) suggested using temporal sampling to monitor the evolution of clonal rates through time, but temporal studies are largely lacking. Spatial and temporal sampling may be necessary to resolve the processes that drive reproductive mode variation (Becheler et al., 2017; Halkett et al., 2005) because the reproductive system shapes genetic diversity (Hamrick & Godt, 1996) and drives evolutionary responses to environmental change (e.g., Eckert et al., 2010; Orive et al., 2017).

Several studies on the reproductive system have characterized temporal variation in traditional population genetic summary statistics (e.g., genetic differentiation, genotypic diversity, inbreeding coefficients, linkage disequilibrium) and how those statistics vary with seasons and environmental conditions (Guillemaud et al., 2003; Reynolds et al., 2017; Tibayrenc & Ayala, 2012). For example, some aphids are cyclical parthenogens in which they have periods of asexual reproduction followed by a sexual event, resulting in some genetic variability within years but stability between years (Guillemaud et al., 2003, 2011). This phenomenon is distinct from other types of partial clonality in which sexual and asexual reproduction occur simultaneously. For example, genetic differentiation between years highlights the importance of the banking and continuous germination of resting cysts on the bloom dynamics of microalgae (Dia et al., 2014; Lebret et al., 2012). For diploids, linkage disequilibrium, heterozygosity, and the inbreeding coefficient F_{IS} have often been used as proxies to estimate reproductive modes and their temporal variations (Arnaud-Haond et al., 2007; Allen & Lynch, 2012; Stoeckel & Masson, 2014; Bürkli et al., 2017), although those measures can be inaccurate for low-to-moderate clonal rates and cannot be assessed in the haploid phase. Although these comparative methods can be informative, traditional population genetic summary statistics do not provide direct rates of clonality and selfing.

Reproductive modes can be more directly characterized using dedicated methods to estimate changes in genotypic frequencies through time (Becheler et al., 2017; Stoeckel et al., 2024). These methods require three conditions that can be difficult to meet for non-model species with complex life cycles: (i) prior knowledge of the generation time of natural populations, as samples should be collected one generation apart, (ii) prior knowledge of inbreeding and selfing rates, and (iii) diploid genotypes. Therefore, these methods are difficult, or in some cases impossible, to use for haploid–diploid organisms such as algae, ferns, and some fungi (Becheler et al., 2017). Yet, macroalgae present an opportunity to better understand the evolution of sex because many exhibit spatial and temporal separation of meiosis and fertilization resulting in two phases—often haploid and diploid—of long duration (Otto & Marks, 1996). Algae exhibit a broad diversity of types of life cycles, are phylogenetically diverse, and have, thus, been proposed for testing the influence of life cycles on reproductive system variation (see Krueger-Hadfield et al., 2021; Krueger-Hadfield, 2024; Olsen et al., 2020; Otto & Marks, 1996). Most previous data have been taxonomically restricted to brown algae (see Heesch et al., 2021) and marine red algae (e.g., Engel et al., 1999, 2004; Guillemin et al., 2008; Krueger-Hadfield et al., 2013, 2015; see additionally Krueger-Hadfield et al., 2021). Otto and Marks (1996) proposed green algae as useful models for testing predictions for reproductive system variation across types of life cycle, but there are still too few data to accurately test these hypotheses (see Krueger-Hadfield 2024).

We recently expanded the taxonomic breadth of reproductive system studies to include freshwater red algae (Krueger-Hadfield et al. 2024). Not only do they

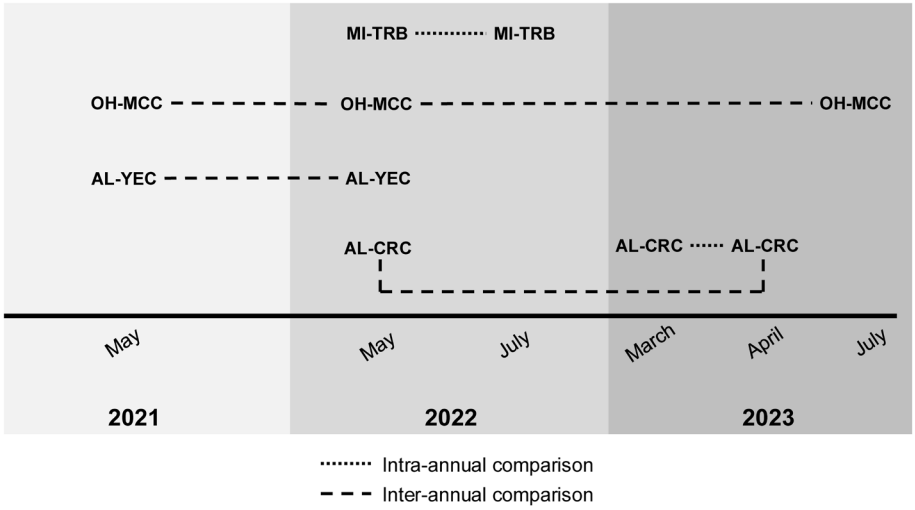

FIGURE 1 Conceptual diagram for the sampling dates at each site, shown in latitudinal order from north to south. Months and years are indicated along the horizontal axis. Shading distinguishes each year. Traverse River on Big Traverse Rd., MI (MI-TRB) was sampled in May 2022 and July 2022 for an intra-annual comparison. Monday Creek, OH (OH-MCC) was sampled in May 2021, May 2022, and July 2023, providing interannual comparisons across 3 years. Yellow Creek, AL (AL-YEC) was sampled in May 2021 and May 2022, for an interannual comparison between 2 years. Cripple Creek, AL (AL-CRC) was sampled in May 2022, March 2023, and April 2023, for both an interannual comparison and an intra-annual comparison.

display variation in their sexual systems (i.e., monoicy and dioicy; see Figure 2 in Krueger-Hadfield et al. 2024), but species in the Batrachospermales have a unique haploid-diploid life cycle in which a microscopic, perennial diploid phase—called the chantransia—alternates with a macroscopic, ephemeral haploid gametophyte phase. Unlike what is observed in the tetrasporophytes of marine red algae, a unique type of meiosis, called vegetative meiosis, occurs at the tip of the chantransia filament in species in the Batrachospermales. This process results in the loss of three nuclei while only the one remaining nucleus remains in the initial cell of the gametophyte, which is physically attached but functionally independent from the chantransia. This life cycle results in unique eco-evolutionary consequences for these types of red algae (see Krueger-Hadfield et al., 2024; see Figure 1 in Shainker-Connelly et al., 2024). First, many species in the Batrachospermales are monoicous, unlike most marine red algae, most of which are dioicous (but see the following exceptions: Fujio et al., 1985; Maggs, 1988; Lindstrom, 1993). As a result, intragametophytic selfing may be common whereby fertilization can occur between a spermatium (male gamete) and a carpogonium (female gamete) produced by the same monoicous gametophyte. This type of selfing results in instantaneous, genome-wide homozygosity, unlike selfing in diploid-dominant or dioicous organisms (Klekowski, 1969; see Figure 1a in Shainker-Connelly et al., 2024). A second type of selfing, intergametophytic selfing, may also be common and describes fertilization between gametes produced by two gametophytes originating from the same parental chantransia. It is possible that one chantransia could produce multiple gametophytes through the occurrence of vegetative meiosis on different filaments of that chantransia. The proximity of these gametophytes arising from the same chantransia could facilitate intergametophytic selfing. Alternatively, monospore production by chantransia will result in many chantransia sharing the same genotype and subsequently producing gametophytes. Both scenarios would be analogous to other algae, such as marine red algae, in which gamete unions occur between morphologically independent gametophytes that share the same sporophytic parent. For example, the high rates of intergametophytic selfing and the clumped dispersal of tetraspores in *Chondrus crispus* (see Krueger-Hadfield et al., 2013, 2015) has been proposed to drive a pattern of discrete genotypes in close proximity to one another (Krueger-Hadfield, 2011). Although intergametophytic selfing in freshwater or marine red algae involves cross-fertilization, the mating between sibs leads to the gradual erosion of genetic diversity in a population. This process is considered a form of selfing because the genetic effects are identical to those of selfing in diploid-dominant organisms (Klekowski, 1969). Finally, the chantransia can reproduce asexually by producing monospores, which germinate and develop into new chantransia (Sheath, 1984; see Figure 1d in Shainker-Connelly et al., 2024). The frequency of monospore production in natural populations is unknown. Moreover, it would be difficult to distinguish between monospore production by a chantransia and different carpospores from the same gametophyte germinating into chantransia, as both would result in many chantransia sharing the same genotype. The life cycle highlights the complications that arise when characterizing the reproductive systems of nonmodel, haploid-diploid taxa and

the necessity of expanding our toolbox to encompass eukaryotic diversity more broadly.

We recently characterized the reproductive system of the monoicous, widespread red alga *Batrachospermum gelatinosum* (Sheath & Cole, 1992; Vis & Necchi Jr., 2021) across eastern North America (Shainker-Connelly et al., 2024). We interpreted the patterns of population genetics we observed as indicative of high rates of intragametophytic selfing, although we noted that we could not distinguish between the genetic effects of intragametophytic selfing and monospore production using haploid gametophytic genotypes. Here, we expand on our previous work by using temporal genotyping to improve our understanding of the reproductive system of *B. gelatinosum*. Four of the sites from our previous study (Shainker-Connelly et al., 2024) were sampled at multiple time points to assess temporal patterns of reproductive system variability (Figure 1, Appendix S1: Figure S1). From previous single-snapshot genotyping, we observed genetic signatures of high rates of intragametophytic selfing at two sites, whereas the other two sites had more intermediate selfing rates (Shainker-Connelly et al., 2024).

We aimed to use interannual population genetic comparisons to better understand the temporal dynamics of the reproductive system (Figure 1). Although changes within a year may result from the seasonality of the life cycle, interannual dynamics may reflect how the reproductive system shifts or remains stable through time. We anticipated the following three scenarios: (1) high rates of intragametophytic selfing may maintain low levels of standing diversity through time, (2) populations may undergo increasing rates of intragametophytic selfing through time as genetic diversity is eroded, or (3) populations may have mixed reproductive systems with intragametophytic selfing, intergametophytic selfing, and outcrossing (i.e., mixed mating, Goodwillie et al., 2005). The population genetic patterns expected to be associated with each scenario are described in Table 1.

We aimed to use intra-annual comparisons (Figure 1) to better understand the seasonality of the haploid-diploid *B. gelatinosum* life cycle. The perennial chantransia likely enhances population stability by persisting through disturbances and maintaining abundance in the upstream reaches (i.e., a smaller section of a stream) of drainage basins (Hambrook & Sheath, 1991). The macroscopic gametophytes typically appear seasonally, although they may be perennial in some cases (Sheath & Vis, 2015). Because these shifts in the life cycle occur within a year, intra-annual sampling may elucidate population genetic patterns driven by the seasonality of the life cycle. We anticipated two potential scenarios: (1) genetically distinct chantransia may produce gametophytes at the same time or (2) genetically distinct chantransia may produce gametophytes at different times throughout the season. The predicted population genetic patterns for each scenario are described in Table 1. Our work provides a reference point for understanding the dynamics of the life cycle and temporal patterns of reproductive system variation in *B. gelatinosum*, thereby expanding our understanding of eukaryotic reproductive system variation. Moreover, this study is one of a handful of attempts to use temporal sampling to characterize population genetic parameters in natural populations.

MATERIALS AND METHODS

Sample collection

We collected *B. gelatinosum* gametophytic thalli (hereafter referred to as gametophytes) from four sites in the eastern United States in 2021, 2022, and 2023 (Table 1, Figure S1). We did not sample the chantransia because they are microscopic, and genotyping would be a challenge (see Schoenrock et al., 2020 for a discussion on microscopic forms). Sites AL-CRC (Alabama) and MI-TRB (Michigan) were each sampled twice within the same season to provide an intra-annual comparison of genotypes: AL-CRC in March 2023 and April 2023 and MI-TRB in May 2022 and July 2022. Sites AL-CRC, AL-YEC (Alabama), and OH-MCC (Ohio) were each sampled during sequential years, providing interannual comparisons of genotypes: AL-CRC in May 2022 and April 2023, AL-YEC May 2021 and May 2022, and OH-MCC in May 2021, May 2022, and July 2023 (Table 2, Figure 1). The sampling protocols were also described in Shainker-Connelly et al. (2024) and Crowell, Shainker-Connelly, Krueger-Hadfield, and Vis (2024). For each site, we used Google Maps or the iPhone app GPSCoordinates ver. 5.18 (Neal, 2018) to note GPS coordinates. We used a transect tape to measure stream width and length of the sampled reach, chosen based on accessibility and the presence of gametophytes. We visually estimated stream bed composition, water color, and water clarity near the middle of the sampling area (Appendix S1: Table S1). At sites AL-CRC, AL-YEC, and MI-TRB (see Table 1), we used an Oakton PCTSTestr 50 Pocket Tester to measure pH, water temperature, and specific conductivity. At OH-MCC, we used an Oakton pHTestr 5 to measure pH and water temperature and an Oakton ECTestr low to measure specific conductivity. We used a flow probe (Global Water Instruments, Model FP111) to measure current velocity and stream depth at sites AL-CRC, AL-YEC, and MI-TRB (see Table 1). At OH-MCC, we used a different flow probe (General Oceanics, Mechanical Flow Meter) and measured stream depth with a ruler. At sites AL-CRC, AL-YEC, and MI-TRB (see Table 1), we used a spherical densiometer (Forest Densiometer, Model A) to calculate percent canopy cover following Lemmon (1956) and Lemmon (1957) but with one

TABLE 1 Summary of temporal comparisons and predictions of potential outcomes for *B. gelatinosum*.

Comparison	Purpose	Sites and time points	Predictions	Genetic patterns
Interannual	Temporal patterns in the reproductive system	OH-MCC • May 2021 • May 2022 • July 2023 AL-YEC • May 2021 • May 2022 AL-CRC • May 2022 • April 2023	High levels of intragametophytic selfing	*LOW DIVERSITY* • *Linkage disequilibrium*: High with low variance • *Genetic diversity*: Consistently low • *Temporal genetic differentiation*: Low • *Genotypic richness and evenness*: Low • *Raw and diverging alleles*: Low
			Increasing intragametophytic selfing from 1 year to the next	*INTERMEDIATE DIVERSITY* • *Linkage disequilibrium*: Increase from year to year • *Genetic diversity*: Decrease from year to year • *Temporal genetic differentiation*: Intermediate to high • *Raw and diverging alleles*: Decrease from year to year
			Mixed mating system	*HIGH DIVERSITY* • *Linkage disequilibrium*: Low with high variance • *Genetic diversity*: Intermediate to high with high variance • *Temporal genetic differentiation*: Intermediate to high with high variance • *Raw and diverging alleles*: Broad distribution
Intra-annual	Seasonality of the life cycle	MI-TRB • May 2022 • July 2022 AL-CRC • March 2023 • April 2023	All gametophytes at the same time of year	*CONSISTENT DIVERSITY* • *Genetic diversity*: Consistent • *Temporal genetic differentiation*: Low • *Genotypic richness and evenness*: Consistent • *Genotypes*: Similar between time points
			Different chantransia genotypes undergo meiosis at different times to produce gametophytes throughout the season	*INCREASING DIVERSITY* • *Genetic diversity*: Increase from one time point to the next • *Temporal genetic differentiation*: High • *Genotypic richness and evenness*: Increase from one time point to the next • *Genotypes*: Transition between time points

reading instead of four. At OH-MCC, canopy cover was estimated by eye.

We haphazardly sampled gametophytes within the measured sampling length of the reach (see Table 2), aiming to collect 20–30 gametophytes from each time point at each site. At some time points, there were few gametophytes with a patchy distribution, resulting in smaller sample sizes (Table 3). The stream we sampled at AL-CRC contains three distinct sections: an upstream riffle, a pool, and a downstream riffle. We took environmental measurements within each of these three distinct sections and noted the sections from which gametophytes were collected. Most *B. gelatinosum* gametophytes were collected in the riffles, so the environmental measurements taken in the upstream riffle section are reported, except for the sampling length, which includes both riffles and the pool (Table 2).

We used a dissecting microscope (40× magnification) to look for carposporophytes on each gametophyte. In our previous work (Crowell, Shainker-Connelly, Krueger-Hadfield, & Vis, 2024; Crowell, Shainker-Connelly, Vis, & Krueger-Hadfield, 2024; Shainker-Connelly et al., 2024), the presence of carposporophytes did not result in "diploid" gametophytes with two or more alleles. This could be due to high rates of intragametophytic selfing in which the same gametophyte produced both the carpogonium (i.e., egg) and spermatium (i.e., sperm) that resulted in the formation of the carposporophyte. Alternatively, DNA from the genotyped gametophyte may have swamped any exogenous paternal DNA in the carposporophytes. We ensured that we preserved a single gametophyte by physically separating thalli if entangled with one another and by removing the lower portion of the thallus to ensure that there were no remnants of the chantransia. We used silica gel (Activa Flower Drying Art Silica Gel) to preserve tissue from each gametophyte. When possible, the remaining thallus was mounted on herbarium paper (University of California-type Herbarium Mounting Paper, Herbarium Supply, Bozeman, MT), and representative vouchers were deposited in the Floyd Bartley Herbarium at Ohio University (Table 2).

DNA extraction and PCR amplification

We extracted total genomic DNA using the Machery-Nagel Nucleospin® Plant II kit (Macherey-Nagel) following the manufacturer's protocol, except that the lysate was incubated at room temperature for 1 h and DNA was eluted in a 100 μL volume of molecular grade water (see also Crowell, Shainker-Connelly, Krueger-Hadfield, & Vis, 2024; Shainker-Connelly et al., 2024).

We used 10 previously developed microsatellite loci (locus development described in Crowell, Shainker-Connelly, Vis, & Krueger-Hadfield, 2024;

TABLE 2 Locations and physiochemical data measured at each site in which *B. gelatinosum* gametophytes were sampled at multiple time points. Dashes (–) indicate that the measurement was not taken.

Site names	Site abbreviations	State	Sampling date	Latitude	Longitude	Herbarium voucher	pH	Specific conductivity ($\mu S \cdot cm^{-1}$)	Water temperature (°C)	Current velocity ($m \cdot s^{-1}$)	Stream depth (cm)	Stream width (m)	Sampling length (m)	Canopy cover (%)
Traverse river on Big Traverse Rd.	MI-TRB	Michigan	12-May-2022	47.195156	−88.239225	BHO: A-1889	7.14	30.9	9.1	0.5	54	7.74	9.44	5.3
			26-Jul-2022			BHO: A-1887	–	–	–	–	–	–	–	–
Monday Creek	OH-MCC	Ohio	19-May-2021	39.500500	−82.246300	BHO: A-1723	6.62	500	17.1	–	42	11.1	18	50
			5-May-2022			BHO: A-1814	8.0	510	16.2	0.3	70	7	40	20
			23-Jul-2023			BHO: A-1993	7.3	580	21.2	0.18	38	8.3	18	90
Yellow Creek	AL-YEC	Alabama	19-May-2021	33.572000	−87.403000	BHO: A-1902	7.06	151	19.5	0.4	50	5.65	33.6	18.7
			2-May-2022			BHO: A-2038	7.15	50	18.5	0.8	26	5.01	34.8	-
Cripple Creek	AL-CRC	Alabama	2-May-2022	33.492530	−87.562633	BHO: A-2037	7.34	124	16.5	0.3	17	6.5	45.16	64
			16-Mar-2023			BHO: A-2064	7.41	86.3	7.5	0.6	31	7.3	48	13
			20-Apr-2023			BHO: A-2065	7.22	129.6	13	0.6	17	7.5	48	39

phylogeographic patterns described in Crowell, Shainker-Connelly, Krueger-Hadfield, & Vis, 2024; reproductive system variation from one-shot genotyping described in Shainker-Connelly et al., 2024). We amplified most loci for most gametophytes using multiplex polymerase chain reactions (PCRs) with a final volume of 15 μL: 2 μL of DNA, forward and reverse primers (Appendix S1: Table S2), 1× Promega GoTaq® Flexi Buffer (Promega, Madison, WI, USA; Cat #M890A), 2 mM of $MgCl_2$ (Promega, Madison, WI, USA; Cat #A351H), 250 μM of each dNTP (Promega, Madison, WI, USA; Cat #R0192), 1 mg · mL^{-1} of BSA, and 1.0 U of Promega GoTaq® Flexi DNA Polymerase (Promega, Madison, WI, USA; Cat #M829B). For the locus Bgel_056, we used simplex PCRs with a final volume of 15 μL: 2 μL of DNA, 150 nM of the forward labeled primer, 100 nM of the forward unlabeled primer, 250 nM of the unlabeled reverse primer, 1c buffer (Promega, Madison, WI, USA; Cat #M890A), 2 mM of $MgCl_2$, 250 μM of each dNTP (Promega, Madison, WI; Cat #R0192), 1 mg · mL^{-1} of BSA, and 1U of Promega GoTaq® Flexi DNA Polymerase (Promega, Madison, WI, USA; Cat #M829B). For reruns of any loci that did not amplify in the first attempt in a multiplex PCR, we used simplex PCRs with final volumes of 15 μL: 2 μL of DNA, 250 nM of the forward labeled primer, 250 nM of the unlabeled reverse primer, 1× buffer (Promega, Madison, WI, USA; Cat #M890A), 2 mM of $MgCl_2$, 250 μM of each dNTP (Promega, Madison, WI; Cat #R0192), 1 mg/mL of BSA, and 1 U of Promega GoTaq® Flexi DNA Polymerase (Promega, Madison, WI, USA; Cat #M829B). We used the following PCR program: 95°C for 2 min, followed by 35 cycles of 95°C for 30 s, 59°C for 30 s, and 72°C for 30 s, with a final extension stage of 72°C for 5 min.

We diluted 1.5 μL PCR product in 9.7 μL HiDi formamide (Applied Biosystems, Cat #4311320) and 0.30 μL GS 500 LIZ (Applied Biosystems, Cat #4322682). Fragment analysis was then performed at the Heflin Center for Genomic Sciences at the University of Alabama at Birmingham. We scored alleles using Geneious Prime v.2022.2.2 (https://www.geneious.com), then manually checked each bin with those previously described in Crowell, Shainker-Connelly, Vis, and Krueger-Hadfield (2024), adjusting when the raw allele size was slightly larger or smaller than the previously defined bins (Appendix S1: Table S3).

After several PCR attempts, locus Bgel_071 did not amplify for most gametophytes sampled at all three time points at OH-MCC. This result was consistent with a geographic pattern previously detected at this site (Crowell, Shainker-Connelly, Krueger-Hadfield, & Vis, 2024; Shainker-Connelly et al., 2024). Bgel_071 was removed from OH-MCC gametophytes, so a total of nine loci were used for analyses of all time points at this site.

Data analyses

Gametophytes for which any loci did not amplify after several PCR attempts were excluded from subsequent analyses. The null allele frequency was directly estimated by calculating the percent of gametophytes that did not amplify at each locus after several PCR attempts and after discounting technical errors (see also Krueger-Hadfield et al., 2011).

We calculated the following multilocus summary statistics for each time point at each site to describe the reproductive system, following the recommendations and methods described by Stoeckel et al. (2021) and implemented in Krueger-Hadfield et al. (2021). We calculated the probability of identity between sibs (*pid*), which ranges from 0 to 1, to assess whether loci were of sufficient resolution to distinguish between distinct genotypes (Jacquard, 2012; Waits et al., 2001). Then, we calculated genotypic richness (*R*), which provides information on the relative proportion of repeated multilocus genotypes (MLGs), as: $R = \frac{(G-1)}{(N-1)}$, where *G* is the number of distinct genotypes (i.e., genets), and *N* is the number of genotyped gametophytes (Dorken & Eckert, 2001). We also calculated genotypic evenness, which provides information about the relative abundance of each MLG in a site (D^*, see box 3 in Arnaud-Haond et al., 2007) and is expected to increase with increasing *R* in outcrossed populations (Baums et al., 2006; Krueger-Hadfield et al., 2021).

We calculated multilocus and per-locus values of expected heterozygosity (H_E) following Stoeckel et al. (2021). To calculate mean allelic richness for each time point, we used the allelic richness function in the R package hierfstat (Goudet & Jombart, 2015). We then described the distribution of clonal membership (Pareto β) for each time point sampled (Table 3). As *B. gelatinosum* is monoicous, intragametophytic selfing and asexual reproduction result in similar population genetic patterns, so Pareto β cannot be used to disentangle the effects of these two reproductive modes (see Shainker-Connelly et al., 2024). We considered that Pareto $\beta > 2$ was associated with low rates of intragametophytic selfing, $0.7 <$ Pareto $\beta < 2$ was associated with intermediate rates of intragametophytic selfing, and Pareto $\beta < 0.7$ was associated with high rates of intragametophytic selfing, following similar predictions for asexual reproduction based on empirical data in Krueger-Hadfield et al. (2021).

For each time point at each site, we calculated multilocus values of linkage disequilibrium ($\bar{r}_d$) following Agapow and Burt (2001). We also determined linkage disequilibrium ($|D'|$) between each pair of alleles for each time point (Lewontin, 1964). In partially clonal taxa, including red macroalgae, both asexual reproduction and selfing can lead to an increase in $\bar{r}_d$ and pairwise $|D'|$ values and variance of these

TABLE 3 Summary statistics calculated for sites in which *B. gelatinosum* gametophytes were sampled at multiple time points, with site abbreviations indicated (see Table 1). The third column ("Intra" or "inter") indicates whether the time point was used for an interannual comparison, an intra-annual comparison, or both. Ten microsatellite loci were used for all sites except OH-MCC, for which nine microsatellite loci were used because locus Bgel_071 did not amplify. Summary statistics include the following: *n*, total number of gametophytes genotyped; *G*, number of unique genotypes; *pid*, probability of identity of sibs; *R*, genotypic richness; *D**, genotypic evenness; Pareto ß, distribution of clonal membership, H_E, expected heterozygosity $\overline{r_d}$, multilocus estimate of linkage disequilibrium; and the number of fixed loci per sampling date.

Site abbreviations	Sampling dates	*n*	*G*	*pid*	*R*	*D**	H_E	Pareto ß	$\overline{r_d}$	Number of fixed loci	Mean allelic richness
Interannual comparisons											
OH-MCC	19-May-2021	20	1	1.000	0.00	0.00	0.000	0.02	1.00	9	1.00
	5-May-2022	28	2	0.666	0.04	0.07	0.015	0.01	1.00	7	1.15
	23-Jul-2023	19	1	1.000	0.00	0.00	0.000	0.02	1.00	9	1.00
AL-YEC	19-May-2021	17	5	0.150	0.25	0.43	0.064	0.10	0.29	7	1.20
	2-May-2022	22	3	0.285	0.10	0.56	0.058	0.16	0.03	8	1.13
AL-CRC	2-May-2022	27	15	0.004	0.54	0.88	0.159	0.49	0.04	4	1.49
	20-Apr-2023[a]	25	11	0.012	0.42	0.89	0.159	0.66	0.04	5	1.42
Intra-annual comparisons											
MI-TRB	12-May-2022	6	4	2.17E-05	0.60	0.80	0.344	0.63	0.66	2	2.30
	26-Jul-2022	13	6	4.76E-05	0.42	0.64	0.308	0.23	0.50	2	1.97
AL-CRC	16-Mar-2023	14	8	0.002	0.54	0.89	0.190	0.84	0.20	4	1.60
	20-Apr-2023[a]	25	11	0.012	0.42	0.89	0.159	0.66	0.04	5	1.42

[a]Samples from this time point were used for both inter- and intra-annual comparisons.

TABLE 4 The raw number of alleles counted at each locus, for each sampling point, is provided. A dash (–) is entered for locus Bgel_071 at all time points at OH-MCC since this locus did not amplify for the gametophytes sampled at this site.

Site abbreviations	Sampling dates	Bgel_021	Bgel_071	Bgel_052	Bgel067	Bgel_053	Bgel_070	Bgel_059	Bgel_073	Bgel_057	Bgel_056
MI-TRB	12-May-2022	1	4	2	1	3	2	2	2	3	3
	26-Jul-2022	1	4	2	1	3	5	2	2	3	3
OH-MCC	19-May-2021	1	–	1	1	1	1	1	1	1	1
	5-May-2022	2	–	2	1	1	1	1	1	1	1
	23-Jul-2023	1	–	1	1	1	1	1	1	1	1
AL-YEC	19-May-2021	2	3	2	1	1	2	1	1	1	1
	2-May-2022	1	2	1	1	1	1	1	1	1	2
AL-CRC	2-May-2022	1	6	1	2	2	2	1	1	2	2
	16-Mar-2023	1	4	1	2	3	2	1	1	2	2
	20-Apr-2023	1	6	1	2	2	2	1	1	1	2

values within a species (Krueger-Hadfield et al., 2021; Stoeckel et al., 2021).

To measure genetic differentiation between time points at the same site, we calculated a pairwise measure of temporal genetic differentiation, like F_{ST}, for each locus. This value ranges from 0 to 1, where 0 refers to no differentiation, and 1 refers to fixation of different alleles. Finally, we calculated raw genetic distances for all pairs of gametophytes using GenAPoPop (Stoeckel et al., 2024) adapted for haploid data. The maximum possible number of diverging alleles between a pair of gametophytes was 10 for all sites except OH-MCC. As Bgel_071 was excluded for OH-MCC, the maximum possible number of diverging alleles between pairs of gametophytes at all time points was nine at OH-MCC. We calculated the number of diverging alleles between all pairs of gametophytes for each site within each sampled time point. Finally, we calculated the number of raw alleles present at each locus (Table 4).

Data visualization

Figures were prepared using R ver. 2022.07.2 (R Core Team, 2022) with the following packages: ggplot2 (Wickham, 2016), gridExtra (Auguie, 2017), pastecs (Grosjean & Ibanez, 2018), and car (Fox & Weisberg, 2019).

RESULTS

Genotyping and null alleles

We generated a total of 191 gametophytic genotypes. We attempted to amplify all loci for 208 gametophytes from four sites collected at 10 different time points. One gametophyte did not amplify at locus Bgel_021, five at Bgel_067, one at Bgel_053, four at Bgel_059, and 10 at Bgel_057. All gametophytes amplified at loci Bgel_052, Bgel_070, Bgel_073, and Bgel_056. Locus Bgel_071 displayed a geographic pattern of non-amplification, in which 65 out of 68 gametophytes from OH-MCC (Ohio) had what we presumed were one or more null alleles, possibly due to an insertion or deletion in the sequence between the locus-specific primers (Crowell, Shainker-Connelly, Krueger-Hadfield, & Vis, 2024; Crowell, Shainker-Connelly, Vis, & Krueger-Hadfield, 2024; Shainker-Connelly et al., 2024). At locus Bgel_071, null allele frequency reached 31.3% when OH-MCC was included, but all gametophytes from other sites amplified at this locus (Appendix S1: Table S4). Excluding Bgel_071, null allele frequencies were low overall (less than 4.8%; Table S4). After 17 gametophytes with one or more loci that did not amplify were removed, 191 gametophytic genotypes remained. The probability of identity (*pid*) was -7.55×10^{-9} over all 124 samples

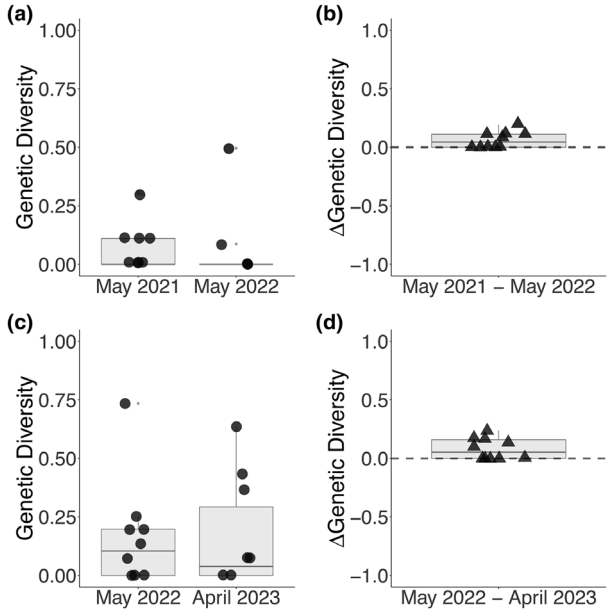

FIGURE 2 The distribution of genetic diversity (calculated as expected heterozygosity, HE) for each locus for interannual time points at (a) Yellow Creek (AL-YEC) and (c) Cripple Creek (AL-CRC). The y-axis range is shown from 0 to 1 for genetic diversity values in (a) and (c). Changes in genetic diversity (shown as ΔGenetic Diversity) between years for each locus are shown for (b) Yellow Creek (AL-YEC) and (d) Cripple Creek (AL-CRC). The *y*-axis range is shown as –1.0 to 1.0 for the change in genetic diversity estimates per locus in (b) and (d), with a dashed gray line to indicate the *y*-intercept at 0. Boxes represent the interquartile range, the middle lines are medians, the whiskers represent the 1.5 interquartile ranges, and the small light gray dots represent outliers.

genotyped at 10 loci (sites AL-CRC, AL-YEC, Alabama and MI-TRB, Michigan), and 0.842 overall 67 samples genotyped with nine loci (site OH-MCC).

Interannual comparisons

Among time points, *pid* values for each set of site-level samples remained stable at a site. At OH-MCC, *pid* ranged from 0.666 in May 2022 to 1 in May 2021 and July 2023. At AL-YEC, *pid* ranged from 0.150 in May 2021 to 0.285 in May 2022. At AL-CRC, *pid* ranged from 0.004 in May 2022 to 0.012 in April 2023 (Table 3).

Genotypic richness and evenness varied among sites but remained stable between interannual time points sampled from a site. At OH-MCC, genotypic richness (*R*) ranged from 0.00 to 0.04, while genotypic evenness (*D**) ranged from 0.00 to 0.07 (Table 3). One multilocus genotype (MLG) was shared among all time points, and one MLG was represented by a single gametophyte in May 2022. At AL-YEC, *R* decreased slightly from 0.25 in May 2021 to 0.10 in May 2022, whereas *D** increased slightly from 0.43 in May 2021 to 0.56 in May 2022 (Table 3). One MLG was shared among 13 and nine gametophytes from May 2021 and May 2022, respectively. Four unique MLGs were represented in May 2021, and one unique MLG in May 2022. At AL-CRC, *R* decreased slightly from 0.54 in May 2022 to 0.42 in April 2023, whereas *D** remained stable at 0.88 in May 2022 and 0.89 in April 2023 (Table 3). Six MLGs were repeated between years, nine MLGs were unique to May 2022, and four MLGs were unique to April 2023.

Among interannual time points at the same site, genetic diversity, measured as expected heterozygosity (H_E), was stable and low (Figure 2). At OH-MCC, H_E ranged from 0.000 to 0.015. Single-locus H_E values at this site were all 0.000 in May 2021 and July 2023. In May 2022, all loci except two (with $H_E = 0.069$) had genetic diversity values of 0.000, for a mean and standard error of 0.015 ± 0.010 at that time point (Table 3). Due to these two loci, the change in H_E ranged from −0.069 to 0.069 over both intervals, whereas the remaining seven loci remained consistent. At AL-YEC, H_E was 0.064 in May 2021 and 0.058 in May 2022. The single locus genetic values ranged from 0.000 to 0.300 in May 2021 with a mean and standard error of 0.064 ± 0.031. In May 2022, the single locus values ranged from 0.000 to 0.500 with a mean and standard error of 0.058 ± 0.049. The genetic diversity for five loci remained consistent among time points, but increased slightly at three loci slightly and descreated at one. Differences in genetic diversity among interannual time points for each locus ranged from −0.191 to 0.111. At AL-CRC, H_E values were the same in May 2022 and April 2023 ($H_E = 0.159$). In May 2022, the single-locus values ranged from 0.000 to 0.740 with a mean and standard error of 0.159 ± 0.071. In April 2023, the single-locus values ranged from 0.000 to 0.640 with a mean and standard error of 0.159 ± 0.073. The genetic diversity remained consistent between time points for four loci, decreased for three loci, and increased for three loci. Differences in genetic diversity among interannual time points for each locus ranged from 0.000 to 0.238 (Figure 2, Table 3). Allelic richness was also low among all interannual time points, ranging from 1.00 (May 2021 and July 2023 at OH-MCC) to 1.49 (May 2022 at AL-CRC; Table 3).

All interannual values of Pareto β were < 0.7. Pareto β values were 0.01–0.02 at OH-MCC, 0.10–0.16 at AL-YEC, and 0.49–0.66 at AL-CRC (Table 3). Multilocus linkage disequilibrium ($\bar{r}_d$) ranged from 0.03 to 1.00 among sites and exhibited a greater amount of variation among sites than between time points sampled at a single site (Table 3). At OH-MCC, $|D'|$ could not be calculated for May 2021 and July 2023 because all loci were fixed. There were 53 comparisons from May 2022. All except four pairs had a $|D'|$ of 0.00. The remaining four range from 0.04 to 0.96 with a mean and standard error of 0.06 ± 0.03. At AL-YEC, there were 99 pairwise comparisons in May 2021, with a range of 0.00–0.94

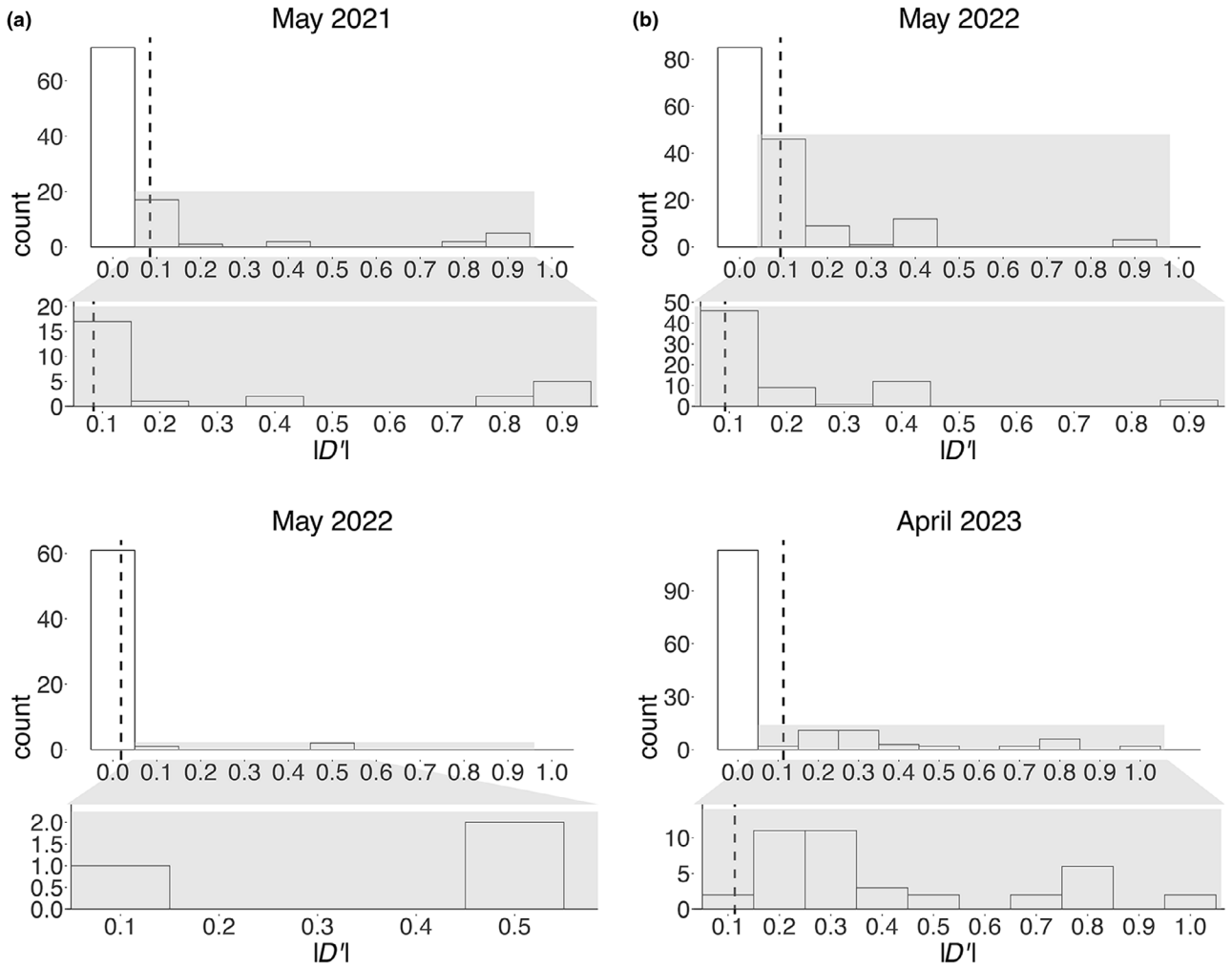

FIGURE 3 The discretized distribution of pairwise linkage disequilibrium (|*D*′|) values per locus are shown for interannual time points in (a) Yellow Creek (AL-YEC) and (b) Cripple Creek (AL-CRC). The *x*-axis indicates discretized linkage disequilibrium values by 0.1 intervals from 0.0 to 1.0 and the *y*-axis ("count") indicates the number of loci with a given |*D*′| range of values. Black dashed lines indicate the mean |*D*′| value. The |*D*′|value was 0.0 when both alleles in a pair were the same.

and a mean and standard error of 0.08 ± 0.02. In May 2022, there were 64 pairwise comparisons with a range of 0.00–0.55 and a mean and standard error of 0.02 ± 0.01. At AL-CRC, there were 156 pairwise comparisons in May 2022 with a range of 0.00–0.85 and a mean and standard error of 0.09 ± 0.01. In April 2023, there were 152 pairwise comparisons with a range of 0.00–0.96 and a mean and standard error of 0.11 ± 0.02 (Figure 3, Appendix S1: Table S5).

For each site, we could not calculate values of temporal genetic differentiation for most pairs of loci due to a lack of allelic variation. Those pairs that could be calculated were close to zero, suggesting little differentiation among interannual time points (Figure 4, Appendix S1: Table S6).

At AL-CRC, there were fewer fixed alleles compared to OH-MCC and AL-YEC (Table 3). At OH-MCC, there were no diverging alleles between most pairs because all except two gametophytes from May 2022 belonged to the same MLG. At AL-CRC, the range (0–4) and mean (~1.5) of diverging allele counts remained consistent at both time points. Additionally, at locus Bgel_071, there was an increase in the raw number of alleles from one year to the next (Table 3). At AL-YEC, the diverging alleles distribution ranged from 0 to 4 in May 2021 and from 0 to 1 in May 2022. However, the mean (~0.5) remained consistent between time points because most pairs in May 2021 exhibited either 0 or 1 diverging alleles (Figure 5).

Intra-annual comparisons

The *pid* values remained consistent within intra-annual time points sampled at the same site. At MI-TRB, *pid* ranged from 2.17×10^{-5} in May 2022 ($n = 6$) to 4.76×10^{-5} in July 2022 ($n = 13$). At AL-CRC, *pid* ranged from 0.002 in March 2023 to 0.012 in April 2023 ($n = 25$). At AL-CRC, *pid* ranged from 0.004 in May 2022 to 0.012 in April 2023 (Table 3).

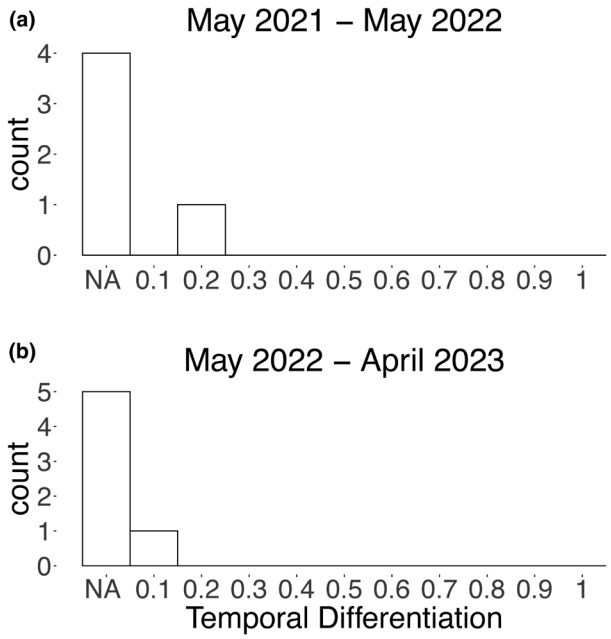

FIGURE 4 The distribution of temporal differentiation is shown for interannual time points in (a) Yellow Creek (AL-YEC) and (b) Cripple Creek (AL-CRC). The *x*-axis indicates temporal differentiation (measured as F_{ST} between time points for each locus; ranges from 0 to 1), and the *y*-axis ("count") indicates the number of loci with a given temporal differentiation range of values. If the expected heterozygosity (H_E) for a locus at both time points was "0," then the pairwise temporal differentiation is indicated as "NA"—not applicable—as differentiation could not be calculated.

Genotypic richness and evenness were stable between time points. At MI-TRB, genotypic richness (*R*) decreased slightly from 0.60 in May 2022 to 0.42 in July 2022, whereas *D** also decreased slightly from 0.80 in May 2022 to 0.64 in July 2022 (Table 3). No MLGs were repeated between both time points. At AL-CRC, *R* decreased slightly from 0.54 in March 2023 to 0.42 in April 2023, whereas *D** remained consistent at 0.89 at both time points (Table 3). Three MLGs were shared between time points, five unique MLGs were sampled only in March 2023, and four unique MLGs were sampled only in April 2023.

Site MI-TRB had slightly greater genetic diversity (H_E) compared to AL-CRC. Between intra-annual time points at a site, H_E was stable and low (Table 3). At MI-TRB, single locus genetic diversity values ranged from 0.000 to 0.670 in May 2022, with a mean and standard error of 0.344 ± 0.070. In July 2022, single-locus H_E values ranged from 0.000 to 0.500 with a mean and standard error of 0.308 ± 0.057. Two loci remained consistent between time points, two decreased, and six increased (Figure 6). At AL-CRC, H_E was 0.159–0.190 (Table 3). Single-locus values ranged from 0.000 to 0.700 in March 2023 with a mean and standard error of 0.190 ± 0.073. In April 2023, single-locus values ranged from 0.000 to 0.630 with a mean and standard error of 0.159 ± 0.073. Values for four loci remained consistent between time points, two decreased, and four increased (Figure 6). Site MI-TRB also had slightly higher mean allelic richness compared to AL-CRC, with values of 2.30 in May 2022 and 1.97 in July 2022, whereas AL-CRC had values of 1.60 in March 2023 and 1.42 in April 2023 (Table 3).

The Pareto β values at both sites decreased between intra-annual time points: at MI-TRB, from 0.63 in May 2022 to 0.23 in July 2022, and at AL-CRC, from 0.84 in March 2023 to 0.66 in April 2023 (Table 3). Multilocus linkage disequilibrium ($\bar{r}_d$) values decreased slightly between intra-annual time points at both sites: from 0.66 to 0.50 at MI-TRB and from 0.20 to 0.04 at AL-CRC (Table 3). Pairwise values of linkage disequilibrium among alleles ($|D'|$) were also calculated. At MI-TRB, there were 234 pairwise comparisons for May 2022, with a range of 0.00–0.83 and a mean and standard error of 0.40 ± 0.02. There were 297 pairwise comparisons for July 2022, with a range of 0.00–0.92 and a mean and standard error of 0.36 ± 0.02. For most loci, $|D'|$ decreased rather than increased through time. At AL-CRC, there were 173 pairwise comparisons in March 2023, with a range of 0.00–0.86 and a mean and standard error of 0.17 ± 0.02. For April 2023, there were 152 pairwise comparisons with a range of 0.00–0.96, and a mean and standard error of 0.11 ± 0.02. The mean $|D'|$ value slightly decreased through time for both sites (Figure 7, Table S5).

We assessed genetic differentiation between intra-annual time points by calculating pairwise values for each locus. At AL-CRC, differentiation could not be calculated between most pairs of loci due to a lack of variation. At MI-TRB, more differentiation values could be calculated. Although genetic differentiation was relatively low between May 2022 and July 2022, values were slightly higher than those that could be calculated between intra-annual time points for AL-CRC and those that could be calculated for interannual time points at all sites (Figures 4 and 8, Table S6).

The number of fixed alleles remained consistent between intra-annual time points sampled at a site. Site MI-TRB had fewer fixed alleles than AL-CRC (Table 3). At both sites, the mean and range of the number of diverging alleles remained consistent between time points, with slight shifts in the distributions. The diverging allele counts implied more genetic variation at MI-TRB than at AL-CRC, but with similar patterns between intra-annual time points within each site (Figure 9).

DISCUSSION

We measured temporal variation in genetic diversity to better assess the reproductive system of *B. gelatinosum*. The *pid* values for sites genotyped with 10 loci indicated that we had sufficient resolution of genotypes,

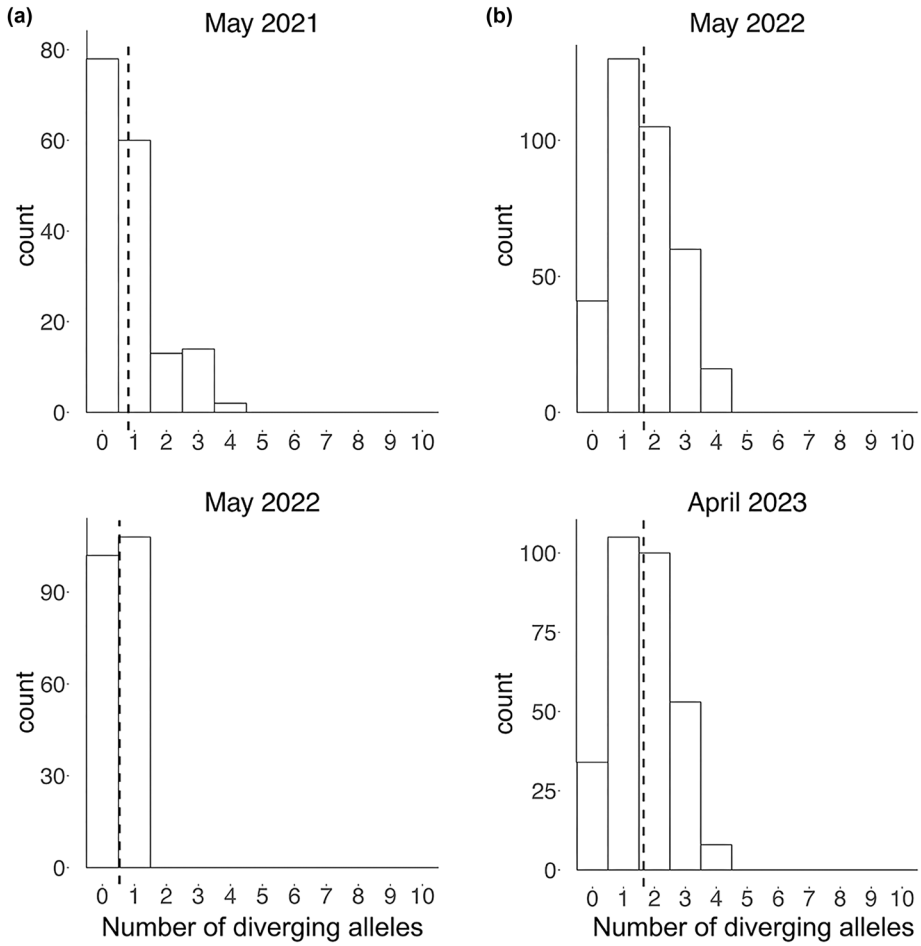

FIGURE 5 The distribution of counts of diverging alleles between each pair of gametophytes are shown for the interannual time points in (a) Yellow Creek (AL-YEC) and (b) Cripple Creek (AL-CRC). The *x*-axis represents the number of diverging alleles from 0 to 10. The y-axis ("count") represents the number of pairs of gametophytes with the given number of diverging alleles. Black dashed lines indicate the mean number of diverging alleles.

but this was not the case for OH-MCC (Ohio). This could be due to high rates of intragametophytic selfing at this site, leading to consistently low diversity. At MI-TRB (Michigan), we surmise there were higher outcrossing rates than the other sites based on greater diversity. Both AL-CRC and AL-YEC (Alabama) had intermediate rates of outcrossing between those observed at MI-TRB (high) and OH-MCC (low, see also Shainker-Connelly et al., 2024). There was little temporal partitioning of genetic variation. Below, we discuss how interannual comparisons inform our knowledge of the reproductive system and how intra-annual comparisons inform our understanding of the seasonality of the *B. gelatinosum* life cycle.

Interannual comparisons: Implications for the reproductive system

At the sites we sampled, the reproductive system of *B. gelatinosum* seemed to remain consistent, with low variation in genetic and genotypic diversity among time points. Low genetic diversity was likely maintained by high rates of intragametophytic selfing, monospore production, or both. We interpret these data as intragametophytic selfing rather than monospore production because we collected gametophytes from all our sampling sites, including those with low genotypic diversity. The presence of gametophytes indicates that meiosis has occurred, as gametophytes are unlikely to result from any clonal processes. Moreover, we have observed very small gametophytes (~1 cm) bearing many carposporophytes (Shainker-Connelly, Crowell, Vis, and Krueger-Hadfield, personal observations). Therefore, fertilization is likely efficient and occurs when gametophytes are very small. Nevertheless, the rates of monospore production by chantransia in natural populations need to be quantified to determine the extent to which clonality contributes to the patterns we observed.

The results of interannual comparisons at site OH-MCC were consistent with our predictions for low standing levels of genetic diversity associated with high rates of intragametophytic selfing (Table 1). As we sampled

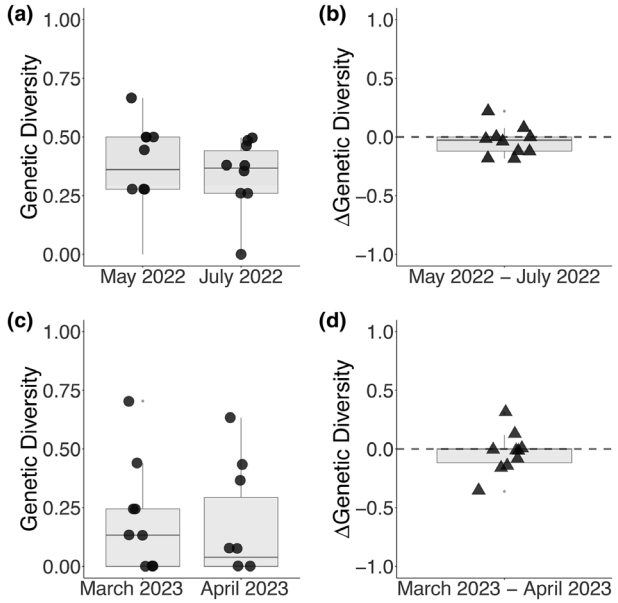

FIGURE 6 The distribution of genetic diversity (calculated as expected heterozygosity, H_E) values at intra-annual time points are shown for (a) Traverse River (MI-TRB) and (c) Cripple Creek (AL-CRC). The *y*-axis range is shown from 0 to 1 for genetic diversity values in (a) and (c). Changes in genetic diversity within years are also indicated for (b) Traverse River (MI-TRB) and (d) Cripple Creek (AL-CRC). The *y*-axis range is shown as –1.0 to 1.0 for the change in genetic diversity estimates per locus in (b) and (d), with a dashed gray line to indicate the *y*-intercept at 0. Boxes represent the interquartile range, the middle lines are medians, the whiskers represent the 1.5 interquartile ranges, and the small light gray dots represent outliers. Boxes represent the interquartile range, the middle lines are medians, the whiskers represent the 1.5 interquartile ranges, and the small light gray dots represent outliers.

one dominant genotype, it is likely that intragametophytic selfing has been maintained long term at this site. The results at site AL-YEC were also consistent with high rates of intragametophytic selfing, although there was likely a slightly higher level of standing genetic diversity than at OH-MCC (Table 1). Although the Pareto β values indicated intragametophytic selfing, the multilocus and single locus values of linkage disequilibrium were both lower at AL-YEC than at OH-MCC. Additionally, the slight decrease in the mean number of diverging alleles from 2021 to 2022 at AL-YEC may have resulted from intragametophytic selfing eroding genetic diversity from only one generation to the next. However, it is also possible that the slight differences observed could be due to chance. It would be necessary to sample additional time points with larger sample sizes, if possible, to determine whether this pattern reflects natural processes or is the result of sampling error. An alternative explanation is that instead of a change in the reproductive system through time, the chantransia that were the product of intragametophytic selfing or monospore production from previous years later produced gametophytes. Future studies would need to genotype chantransia through time to test the feasibility of this explanation.

The results from AL-CRC gametophytes were consistent with our predictions for greater standing genetic diversity with a mixed reproductive system that may include higher rates of outcrossing compared to the other sites. This prediction was supported by the lower *pid* values compared to OH-MCC and AL-YEC, the greater Pareto β values, and a greater mean and wider distribution of the number of diverging alleles. The mixed reproductive system at this site may be driven by greater heterogeneity in biotic and abiotic factors, as a mixed mating system can be stable if there is temporal variation in resource availability (Bengtsson & Ceplitis, 2000; Schemske & Lande, 1985; Weeks, 1993), and environmental fluctuations likely drive reproductive system evolution (Pierre et al., 2022). The microhabitats available at this site are more heterogeneous than at the other sites we sampled in this study. There were two riffles and a pool present within the sampling area, and gametophytes were collected from all these microhabitats, although they were less abundant in the pool than in the riffles. The reproductive mode varies based on microhabitat in other taxa (e.g., water availability, see Johnson & Shaw, 2015), so this variability may have contributed to the patterns observed at AL-CRC. For example, the higher flow velocity in riffles may have facilitated greater fertilization rates than the lower flow velocity in pools. This site was also very diverse in terms of the number of freshwater red algal species observed (Appendix S1: Table S7), and it is possible that there is a relationship between the species diversity and genetic diversity (Vellend & Geber, 2005). Similar selective factors could drive diversification both within and among species, or species diversity may influence the selection regime that drives genetic diversity (Vellend & Geber, 2005). For example, Van Valen (1965) hypothesized that in species-rich communities, the niche breadth of each species would be smaller due to competition, driving a decrease in genetic diversity. Conversely, Harper (1977) predicted that species diversity acts as a source of diversifying selection, so that there is a positive relationship between species and genetic diversity.

Although there were slight differences among sites, the reproductive system likely remains stable through time. Genotyping these sites in future years would be useful to distinguish the time scales at which natural selection may act on the traits that affect the reproductive system. Genotyping chantransia would enable us to measure heterozygosity and quantify clonal rates. Additionally, future studies should investigate sites that likely have lower rates of uniparental reproduction than those included here (e.g., site MI-CUT in Shainker-Connelly et al., 2024). Including sites with lower rates of uniparental reproduction and across more geographic

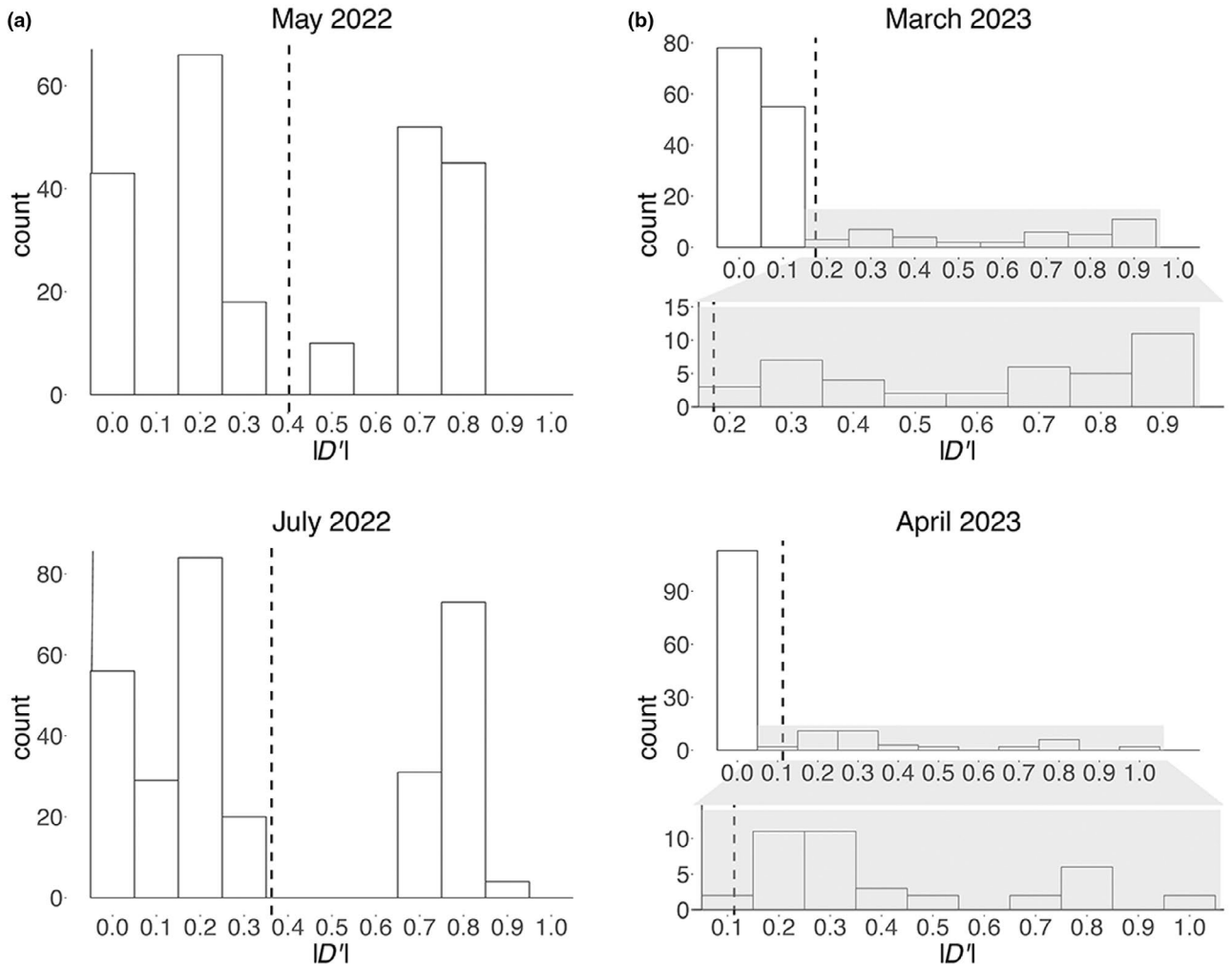

FIGURE 7 The discretized distribution of pairwise linkage disequilibrium (|*D′*|) values per locus are shown for intra-annual time points in (a) Traverse River (MI-TRB) and (b) Cripple Creek (AL-CRC). The *x*-axis indicates per-locus linkage disequilibrium (|*D′*|, ranges from 0 to 1) and the *y*-axis ("count") indicates the number of loci with a given |*D′*| value. Black dashed lines indicate the mean |*D′*| value.

areas would be useful to determine whether stability of the reproductive system is a universal pattern across geographically and genetically distinct sites.

Intra-annual comparisons: Implications for the seasonality of the life cycle

We characterized intra-annual temporal patterns at two sites—MI-TRB and AL-CRC. At both sites, the first sampling point was early in the season when gametophytes were small and patchily distributed throughout the sampled reach. The second sampling point was closer to the peak of gametophytic abundance, when gametophytes were larger and more continuously distributed throughout the sampled reach. Both sites exhibited a slight decrease in linkage disequilibrium between time points, which may be associated with the increase in population size (Waples, 2006) but, alternatively, may be artifacts of sample sizes at the earlier sampling points.

At MI-TRB, no MLGs were shared between time points. In May 2022, the gametophytic subpopulation was small and patchy. Only eight gametophytes were collected and genotyped, from which two were removed because of nonamplification at one locus each. Consequently, it is possible that the sample size at the May time point did not sufficiently capture the genotypes present or possible following meiosis. However, several measures, including allelic richness, genetic diversity, and genotypic richness, suggested that this site is more genetically and genotypically diverse compared to most other *B. gelatinosum* sites (see also Shainker-Connelly et al., 2024). Patterns observed at site MI-TRB were consistent with the prediction that different chantransia genotypes may produce gametophytes at different times, possibly due to environmental changes through the season.

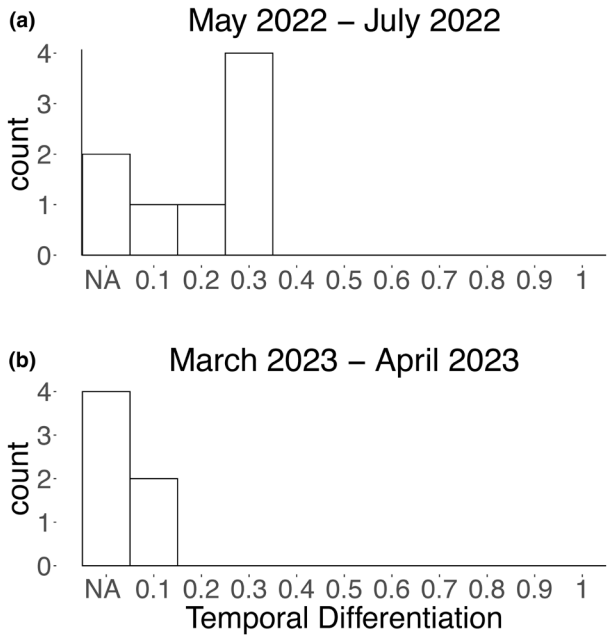

FIGURE 8 The distribution of temporal differentiation is shown for intra-annual time points in (a) Traverse River (MI-TRB) and (b) Cripple Creek (AL-CRC). The *x*-axis indicates temporal differentiation (measured as F_{ST} between time points for each locus; ranges from 0 to 1) and the *y*-axis ("count") indicates the number of loci with a given temporal differentiation range of values. If the expected heterozygosity (H_E) for a locus at both time points was "0," then the pairwise temporal differentiation is indicated as "NA"—not applicable—as differentiation could not be calculated.

A similar pattern has been observed in microalgal blooms, where genetic changes within seasons are thought to be driven by the germination of resting cysts under different conditions (i.e., variations in temperature; Lebret et al., 2012). Alternatively, there could be a succession of genotypes either adapted to slightly different environmental conditions or stochastically favored by disturbance events throughout the season, as observed in rotifers for which a succession of different clonal groups corresponded with temporal changes in environmental conditions (Gómez et al., 1995).

The population genetic diversity and structure of AL-CRC remained more consistent compared to MI-TRB, with little differentiation between intra-annual time points. Several genotypes were observed at just one time point and not the other, but we did not observe the turnover of MLGs to the same degree as at MI-TRB. It should be noted that the intra-annual time points at AL-CRC were sampled just 1 month apart, whereas MI-TRB was sampled 2 months apart. More genotypic shifts may also occur at AL-CRC if observed over a longer 2-month period; however, in 2023, gametophytes at AL-CRC were no longer present 2 months after our initial time point.

Overall, these results suggest that when making population genetic comparisons between and among sites, it may be important to consider the month of sampling and the length of time in which gametophytes are present. Environmental changes and disturbances throughout the season, such as snow melt in northern sites like MI-TRB (Michigan) and storms with heavy rainfall in southern sites like AL-CRC (Alabama), may drive the genotypic shifts observed. Future studies should aim to sample at finer time scales and to measure both population size and environmental variables to better understand the environmental, genetic, and demographic dynamics of gametophytes through time.

Drivers of temporal genetic structure

Temporal environmental changes can cause shifts in the reproductive system, which in turn shape population genetic structure (Eckert et al., 2010). As habitat disturbance and fragmentation increase, plants tend to shift toward higher rates of inbreeding and more variable outcrossing rates (Coates et al., 2013; Eckert et al., 2010). Additionally, it is likely advantageous for both sexual and asexual reproduction to be maintained when conditions are environmentally variable, and the proportion of each type of reproduction may vary temporally as environmental conditions change (Bengtsson & Ceplitis, 2000). For example, both microalgal blooms (Lebret et al., 2012) and cyclical parthenogens, such as potato-peach aphids (Guillemaud et al., 2003), have mixed reproductive modes in which asexual reproduction occurs throughout the year and sexual reproduction may occur once per year. In these situations, there are intra-annual shifts in population genetic structure driven by cyclical reproductive modes, but a stable mixed reproductive mode is maintained long term (Guillemaud et al., 2003; Lebret et al., 2012). It is possible that a similar pattern occurs in freshwater red algae. A stable mixed reproductive mode may be maintained, in which the chantransia reproduce asexually via monospore production throughout the year, meiosis occurs during one season to produce gametophytes, and then fertilization only occurs during the season in which gametophytes are present. Future studies could assess the niche differences between chantransia and gametophytes to determine whether monospore production is favored by certain environmental conditions.

Although there was little interannual variation in our study, there were more differences in genotypes between intra-annual time points, especially at MI-TRB. This pattern is more likely driven by the seasonality of the life cycle rather than the reproductive system. Chantransia are likely present throughout the year, but gametophytes are typically present only during a specific season. These shifts may be driven by the environment. For example, gametophyte cover may be positively correlated with stream depth, current velocity,

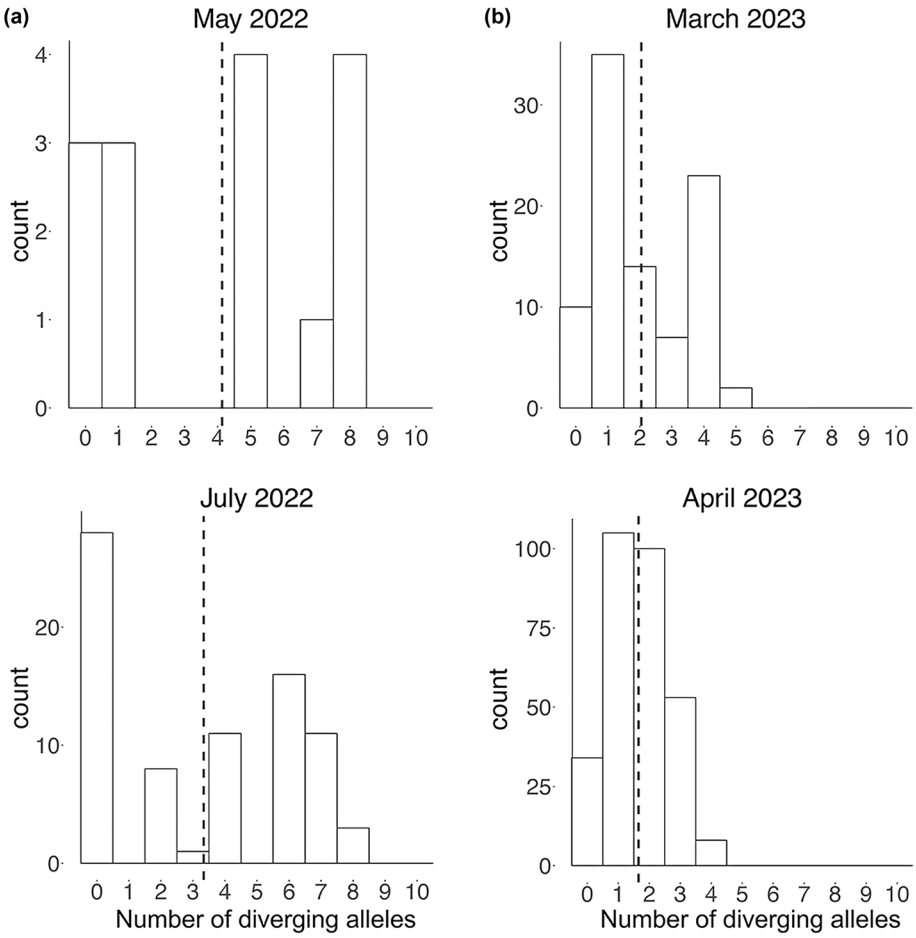

FIGURE 9 The distribution of counts of diverging alleles between each pair of gametophytes collected at intra-annual time points in (a) Traverse River (MI-TRB) and (b) Cripple Creek (AL-CRC). The *x*-axis represents the number of diverging alleles. The *y*-axis ("count") represents the number of pairs of gametophytes with the given number of diverging alleles. Black dashed lines indicate the mean number of diverging alleles.

and day length (Drerup & Vis, 2014), as well as substratum type (Hambrook & Sheath, 1991; Higa et al., 2007), and the timing of gametophytic reproductive maturity may be influenced by light availability and current velocity (Filkin & Vis, 2004). Additionally, chantransia may act as repositories for genetic diversity between seasons. In the bloom-forming microalga *Gonyostomum semen*, fertilization resulted in resting cysts that lay dormant in sediment through the winter (Figueroa & Rengefors, 2006). In the spring, those cysts germinated, and differences in environmental conditions may have been selected for the germination of different genotypes (Lebret et al., 2012). Chantransia may act as a similar repository of genetic diversity by providing a persistent "bank of microscopic forms" (Chapman, 1987; Hoffmann & Santelices, 1991; Schoenrock et al., 2020). It is possible that (i) different chantransia genotypes undergo meiosis to produce gametophytes under different environmental conditions and (ii) different gametophytic genotypes reach reproductive maturity under different environmental conditions. To better understand the putative role of the chantransia phase as a repository for genetic diversity, future studies should determine the lifespan of this phase (i.e., if chantransia thalli persist through multiple gametophyte seasons), the rate of reproduction via monospores, and the environmental factors that may trigger chantransia to undergo meiosis to produce gametophytes.

Methodological limitations and future directions

Our data have provided an overview of temporal patterns of population genetic diversity and structure and have resulted in identifying future avenues to explore in order to understand this freshwater red macroalga better. However, the population genetic tools needed to directly quantify clonal and sexual rates from the haploid phase of haploid-diploid organisms have not yet been developed. In fact, there is generally a lack of standardization in studies that assess clonal rates (Arnaud-Haond et al., 2007). Previous work (e.g., Lebret et al., 2012; Reynolds et al., 2017) has relied on

traditional genetic summary statistics, such as genetic differentiation (F_{ST} measured between time points rather than between sites), genotypic diversity (R), inbreeding coefficient (F_{IS}), and linkage disequilibrium ($\bar{r}_d$), to characterize the reproductive system. These statistics may be used as a proxy for clonal rates, but they are inaccurate for low to moderate clonal rates and do not disentangle the effects of intragametophytic selfing from asexual processes (Shainker-Connelly et al., 2024; Stoeckel et al., 2021). Additionally, F_{IS} can only be calculated in the diploid phase. Here, we have built upon previous studies by incorporating single-locus values of these indices and considering their variance, which can be indicative of partial clonality (Stoeckel et al., 2021). We also incorporated measures of Pareto β, which can be used as a proxy for asexual reproduction and/or intragametophytic selfing (Arnaud-Haond et al., 2007). Future studies could distinguish between selfing and monospore production by using paternity analyses (e.g., Engel et al., 1999; Krueger-Hadfield et al., 2015) to directly assess rates of intra- and inter-gametophytic selfing. This is difficult with traditional methods due to the diminutive size of the carposporophytes in this taxon but is becoming more accessible as advancements in molecular biology allow for the affordable genotyping of single cells and very small amounts of tissue (e.g., Börgstrom et al., 2017; Bowers et al., 2022).

Temporal genotyping may improve assessments of the reproductive system in partially clonal organisms. Becheler et al. (2017) developed methods to directly estimate clonal rates by calculating genotypic transitions between two separate time steps, but at present these methods are only suitable for diploid genotypes. Therefore, without modifying the model of the life cycle in this method, it would be necessary to sample and genotype the chantransia. Sampling the chantransia phase and performing single-cell genotyping would allow for directly estimating clonal rates and the proportion of diploid chantransia to haploid gametophytes in the population. The proportion of haploids has profound consequences for the distribution of population genetic indices and calculation of clonal rates (Stoeckel et al., 2021). However, it is still difficult to collect morphologically separate chantransia because they are microscopic. Developing new methods to directly assess clonal rates from the temporal sampling of haploids may thus be more pragmatic for *B. gelatinosum*. Developing such methods, as has recently achieved for polyploids (e.g., Stoeckel et al., 2024), will allow us to examine both spatial and temporal population genetic patterns across organisms with diverse types of life cycles.

Our results suggest that the reproductive system remains consistent for short-time scales and that the life cycle of *B. gelatinosum* may drive genetic shifts within a season. The development of novel analytical tools, paired with finer-scale temporal sampling, will improve our characterization of how the reproductive system and life cycle drive population genetic patterns. Applying these tools to other freshwater red algal taxa with varying sexual systems (see Krueger-Hadfield et al., 2024) will help us to determine whether patterns are consistent among freshwater reds. Expanding temporal reproductive system studies to include organisms with a wider variety types of life cycle will improve our understanding of the evolution of sex across eukaryotes.

AUTHOR CONTRIBUTIONS

Sarah Shainker-Connelly: Conceptualization (equal); data curation (lead); formal analysis (equal); funding acquisition (supporting); investigation (equal); visualization (equal); writing – original draft (equal); writing – review and editing (equal). **Solenn Stoeckel:** Formal analysis (equal); funding acquisition (supporting); investigation (equal); methodology (equal); software (lead); writing – original draft (supporting); writing – review and editing (equal). **Morgan L. Vis:** Conceptualization (equal); funding acquisition (supporting); investigation (equal); supervision (equal); writing – original draft (supporting); writing – review and editing (equal). **Roseanna M. Crowell:** Funding acquisition (supporting); investigation (equal); writing – review and editing (equal). **Stacy Krueger-Hadfield:** Conceptualization (equal); formal analysis (equal); funding acquisition (lead); investigation (equal); resources (equal); software (supporting); supervision (equal); visualization (supporting); writing – original draft (equal); writing – review and editing (equal).

ACKNOWLEDGMENTS

We thank M. Amsler, B. Anderson, W. Chiasson, A. Oetterer, B. Thornton, S. Thornton, and T. Williams for help collecting *B. gelatinosum*; A. Cao and M. Crowley for use of the capillary sequencer at the Heflin Center for Genomic Sciences at the University of Alabama at Birmingham (UAB); and C. Amsler, M. Sandel, and K. Marion for serving on the dissertation committee of SJSC and providing comments and suggestions that helped improve this manuscript. This manuscript represents the partial fulfillment of the PhD dissertation of SJSC.

FUNDING INFORMATION

This project was supported by the UAB Department of Biology's Harold Martin Outstanding Student Development Award (to SJSC), an Ohio University Student Enhancement Award (to RMC), the Ohio Center for Ecology and Evolutionary Studies Fellowship (to RMC), the Ohio University Roach Fund (to RMC), the Ohio University Graduate Student Senate Original Work Grant (to RMC), Clonix2D ANR-18-CE32-0001 (to SS and SAKH), start-up funds from the College of Arts and Sciences at UAB (to SAKH), and a National

Science Foundation (NSF) CAREER Award (DEB-2141971 to SAKH). SJSC was supported by the UAB Blazer Fellowship and the NSF Graduate Research Fellowship (2020295779). SAKH was supported by the NSF CAREER (DEB-2141971/DEB-2436117), an NSF EAGER award (DEB-2113745), and the Norma J. Lang Early Career Fellowship from the Phycological Society of America. We also thank the Department of Biology at UAB for logistical support.

DATA AVAILABILITY STATEMENT

Shainker-Connelly SJ, S Stoeckel, ML Vis, RM Crowell, SA Krueger-Hadfield (2024) Seasonality and inter-annual stability in the population genetic structure of *B. gelatinosum* (Rhodophyta). Zenodo. https://doi.org/10.5281/zenodo.13835101

ORCID

Sarah Shainker-Connelly https://orcid.org/0000-0003-3403-0294
Solenn Stoeckel https://orcid.org/0000-0001-6064-5941
Morgan L. Vis https://orcid.org/0000-0003-3087-1563
Roseanna M. Crowell https://orcid.org/0000-0003-3117-2094
Stacy A. Krueger-Hadfield https://orcid.org/0000-0002-7324-7448

REFERENCES

Agapow, P. M., & Burt, A. (2001). Indices of multilocus linkage disequilibrium. *Molecular Ecology Notes*, *1*(1–2), 101–102.

Allen, D. E., & Lynch, M. (2012). The effect of variable frequency of sexual reproduction on the genetic structure of natural populations of a cyclical parthenogen. *Evolution*, *66*(3), 919–926. https://doi.org/10.1111/j.1558-5646.2011.01488.x

Arnaud-Haond, S., Duarte, C. M., Alberto, F., & Serrão, E. A. (2007). Standardizing methods to address clonality in population studies. *Molecular Ecology*, *16*(24), 5115–5139.

Auguie, B. (2017). *gridExtra: Miscellaneous functions for "grid" graphics*. R Package Version 2.3.

Barrett, S. C. H. (2011). Why reproductive systems matter for the invasion biology of plants. In D. M. Richardson (Ed.), *Fifty years of invasion ecology: The legacy of Charles Elton* (pp. 195–210). Blackwell Publishing.

Barrett, S. C. H. (2015). IV.8. Evolution of mating systems: Outcrossing versus selfing. In *The Princeton guide to evolution* (pp. 356–362). Princeton University Press.

Baums, I. B., Miller, M. W., & Hellberg, M. E. (2006). Geographic variation in clonal structure in a reef-building Caribbean coral, *Acropora palmata*. *Ecological Monographs*, *76*(4), 503–519.

Becheler, R., Masson, J. P., Arnaud-Haond, S., Halkett, F., Mariette, S., Guillemin, M. L., Valero, M., Destombe, C., & Stoeckel, S. (2017). ClonEstiMate, a Bayesian method for quantifying rates of clonality of populations genotyped at two-time steps. *Molecular Ecology Resources*, *17*(6), e251–e267.

Bengtsson, B. O., & Ceplitis, A. (2000). The balance between sexual and asexual reproduction in plants living in variable environments. *Journal of Evolutionary Biology*, *13*(3), 415–422.

Börgstrom, E., Paterlini, M., Mold, J. E., Frisen, J., & Lundeberg, J. (2017). Comparison of whole genome amplification techniques for human single cell exome sequencing. *PLoS ONE*, *12*(2), e0171566.

Bowers, R. M., Nayfach, S., Schulz, F., Jungbluth, S. P., Ruhl, I. A., Sheremet, A., Lee, J., Goudeau, D., Eloe-Fadrosh, E. A., Stepanauskas, R., Malmstrom, R. R., Kyrpides, N. C., Dunfield, P. F., & Woyke, T. (2022). Dissecting the dominant hot spring microbial populations based on community-wide sampling at single-cell genomic resolution. *ISME Journal*, *16*(5), 1337–1347.

Bürkli, A., Sieber, N., Seppälä, K., & Jokela, J. (2017). Comparing direct and indirect selfing rate estimates: When are population-structure estimates reliable? *Heredity*, *118*(6), Article 6. https://doi.org/10.1038/hdy.2017.1

Chapman, A. R. O. (1987). Population and community ecology of seaweeds. In *Advances in marine biology*, J. H. S. Blaxter and A. J. Southward (Vol. *23*, pp. 1–161). Academic Press.

Coates, D. J., Williams, M. R., & Madden, S. (2013). Temporal and spatial mating-system variation in fragmented populations of *Banksia cuneata*, a rare bird-pollinated long-lived plant. *Australian Journal of Botany*, *61*(4), 235–242.

Crowell, R. M., Shainker-Connelly, S. J., Krueger-Hadfield, S. A., & Vis, M. L. (2024). Population genetics of the freshwater red alga *Batrachospermum gelatinosum* (Rhodophyta) II: Phylogeographic analyses reveal spatial genetic structure among and within five major drainage basins in eastern North America. *Journal of Phycology*, *60*(4), 1437–1455. https://doi.org/10.1111/jpy.13512

Crowell, R. M., Shainker-Connelly, S. J., Vis, M. L., & Krueger-Hadfield, S. A. (2024). Microsatellite development in the freshwater red alga *Batrachospermum gelatinosum* (L.) De Candolle (Batrachospermales, Rhodophyta). *Cryptogamie, Algologie*, *45*(5), 53–62.

Dia, A., Guillou, L., Mauger, S., Bigeard, E., Marie, D., Valero, M., & Destombe, C. (2014). Spatiotemporal changes in the genetic diversity of harmful algal blooms caused by the toxic dinoflagellate *Alexandrium minutum*. *Molecular Ecology*, *23*(3), 549–560.

Dorken, M. E., & Eckert, C. G. (2001). Severely reduced sexual reproduction in northern populations of a clonal plant, *Decodon verticillatus* (Lythraceae). *Journal of Ecology*, *89*(3), 339–350.

Drerup, S. A., & Vis, M. L. (2014). Varied phenologies of *Batrachospermum gelatinosum* gametophytes (Batrachospermales, Rhodophyta) in two low–order streams. *Fottea 14*(2), 121–127.

Drummond, A. J., Pybus, O. G., Rambaut, A., Forsberg, R., & Rodrigo, A. G. (2003). Measurably evolving populations. *Trends in Ecology & Evolution*, *18*(9), 481–488.

Eckert, C. G., Kalisz, S., Geber, M. A., Sargent, R., Elle, E., Cheptou, P. O., Goodwillie, C., Johnston, M. O., Kelly, J. K., Moeller, D. A., Porcher, E., Ree, R. H., Vallejo-Marín, M., & Winn, A. A. (2010). Plant mating systems in a changing world. *Trends in Ecology & Evolution*, *25*(1), 35–43.

Engel, C. R., Destombe, C., & Valero, M. (2004). Mating system and gene flow in the red seaweed *Gracilaria gracilis*: Effect of haploid-diploid life history and intertidal rocky shore landscape on fine-scale genetic structure. *Heredity*, *92*(4), 289–298.

Engel, C. R., Wattier, R., Destombe, C., & Valero, M. (1999). Performance of non-motile male gametes in the sea: Analysis of paternity and fertilization success in a natural population of a red seaweed, *Gracilaria gracilis*. *Proceedings of the Royal Society B: Biological Sciences*, *266*, 1879–1886.

Figueroa, R. I., & Rengefors, K. (2006). Life cycle and sexuality of the freshwater raphidophyte *Gonyostomum semen* (Raphidophyceae). *Journal of Phycology*, *42*(4), 859–871.

Filkin, N. R., & Vis, M. L. (2004). Phenology of *Paralemanea annulata* (Lemaneaceae, Rhodophyta) in an Ohio woodland stream. *Hydrobiologia*, *518*(1–3), 159–168.

Forsström, T., Ahmad, F., & Vasemägi, A. (2017). Invasion genomics: Genotyping-by-sequencing approach reveals regional genetic

structure and signatures of temporal selection in an introduced mud crab. *Marine Biology*, *164*(9), 186.
Fox, J., & Weisberg, S. (2019). *An R companion to applied regression* (3rd ed.). Sage.
Fujio, Y., Kodaka, P. L. G., & Hara, M. (1985). Genetic differentiation and amount of genetic variability in natural populations of the haploid laver *Porphyra yezoensis*. *The Japanese Journal of Genetics*, *60*(4), 347–354.
Gilabert, A., Simon, J. C., Mieuzet, L., Halkett, F., Stoeckel, S., Plantegenest, M., & Dedryver, C. A. (2009). Climate and agricultural context shape reproductive mode variation in an aphid crop pest. *Molecular Ecology*, *18*, 3050–3061.
Gómez, Á., Temprano, M., & Serra, M. (1995). Ecological genetics of a cyclical parthenogen in temporary habitats. *Journal of Evolutionary Biology*, *8*(5), 601–622.
Goodwillie, C., Kalisz, S., & Eckert, C. G. (2005). The evolutionary enigma of mixed mating systems in plants: Occurrence, theoretical explanations, and empirical evidence. *Annual Review of Ecology, Evolution, and Systematics*, *36*, 47–79.
Goudet, J., & Jombart, T. (2015). *Hierfstat: Estimation and tests of hierarchical F-statistics*. R Package Version 0.05-11 https://CRAN.R-project.org/package=hierfstat
Grosjean, P., & Ibanez, F. (2018). *Pastecs: Package for analysis of space-time ecological series*. R Package Version 1.3.21. https://CRAN.R-project.org/package=hierfstat
Guillemaud, T., Blin, A., Simon, S., Morel, K., & Franck, P. (2011). Weak spatial and temporal population genetic structure in the rosy apple aphid, *Dysaphis plantaginea*, in French apple orchards. *PLoS ONE*, *6*(6), e21263.
Guillemaud, T., Mieuzet, L., & Simon, J. C. (2003). Spatial and temporal genetic variability in French populations of the peach-potato aphid, *Myzus persicae*. *Heredity*, *91*(2), 143–152.
Guillemin, M.-L., Faugeron, S., Destombe, C., Viard, F., Correa, J. A., & Valero, M. (2008). Genetic variation in wild and cultivated populations of the haploid–diploid red alga *Gracilaria chilensis*: how farming practices favor asexual reproduction and heterozygosity. *Evolution*, *62*(6), 1500–1519. https://doi.org/10.1111/j.1558-5646.2008.00373.x
Halkett, F., Simon, J. C., & Balloux, F. (2005). Tackling the population genetics of clonal and partially clonal organisms. *Trends in Ecology & Evolution*, *20*(4), 194–201.
Hambrook, J. A., & Sheath, R. G. (1991). Reproductive ecology of the freshwater red alga *Batrachospermum boryanum* Sirodot in a temperature headwater stream. *Hydrobiologia*, *218*(3), 233–246.
Hamrick, J. L., & Godt, M. J. W. (1996). Effects of life history traits on genetic diversity in plant species. *Philosophical Transactions of the Royal Society, B: Biological Sciences*, *351*(1345), 1291–1298.
Harper, J. L. (1977). *Population biology of plants*. Academic Press.
Heesch, S., Serrano-Serrano, M., Barrera-Redondo, J., Luthringer, R., Peters, A. F., Destombe, C., Cock, J. M., Valero, M., Roze, D., Salamin, N., & Coelho, S. M. (2021). Evolution of life cycles and reproductive traits: Insights from the brown algae. *Journal of Evolutionary Biology*, *34*(7), 992–1009. https://doi.org/10.1111/jeb.13880
Higa, A., Kasai, F., Kawachi, M., Kumano, S., Sakayama, H., Miyashita, M., & Watanabe, M. M. (2007). Seasonality of gametophyte occurrence, maturation and fertilization of the freshwater red alga *Thorea okadae* (Thoreales, Rhodophyta) in the Kikuchi River, Japan. *Phycologia*, *46*(2), 160–167.
Hoffmann, A. J., & Santelices, B. (1991). Banks of algal microscopic forms: Hypotheses on their functioning and comparisons with seed banks. *Marine Ecology Progress Series*, *79*(1–2), 185–194.
Jacquard, A. (2012). *The genetic structure of populations* (Vol. *5*). Springer Science & Business Media.
Johnson, M. G., & Shaw, A. J. (2015). Genetic diversity, sexual condition, and microhabitat preference determine mating patterns in *Sphagnum* (Sphagnaceae) peat-mosses. *Biological Journal of the Linnean Society*, *115*(1), 96–113.
Jump, A. S., Hunt, J. M., Martinez-Izquierdo, J. A., & Peñuelas, J. (2006). Natural selection and climate change: Temperature-linked spatial and temporal trends in gene frequency in *Fagus sylvatica*. *Molecular Ecology*, *15*(11), 3469–3480.
Klekowski, E. J. J. (1969). Reproductive biology of the Pteridophyta. II. Theoretical considerations. *Botanical Journal of the Linnean Society*, *62*(3), 347–359.
Krueger-Hadfield, S. A. (2011). Population structure of the haploid-diploid red alga *Chondrus crisps*: reproductive system, genetic differentiation, and epidemiology. [PhD dissertation, Université de Pierre et Marie Curie - Sorbonne Université].
Krueger-Hadfield, S. A. (2024). Let's talk about sex: Why reproductive systems matter for understanding algae. *Journal of Phycology*, *60*(3), 581–597. https://doi.org/10.1111/jpy.13462
Krueger-Hadfield, S. A., Collén, J., Daguin-Thiébaut, C., & Valero, M. (2011). Genetic population structure and mating system in *Chondrus crispus* (Rhodophyta). *Journal of Phycology*, *47*(3), 440–450.
Krueger-Hadfield, S. A., Guillemin, M.-L., Destombe, C., Valero, M., & Stoeckel, S. (2021). Exploring the genetic consequences of clonality in haplodiplontic taxa. *Journal of Heredity*, *112*(1), 92–107.
Krueger-Hadfield, S. A., Roze, D., Correa, J. A., Destombe, C., & Valero, M. (2015). O father where art thou? Paternity analyses in a natural population of the haploid–diploid seaweed *Chondrus crispus*. *Heredity*, *114*(2), 185–194.
Krueger-Hadfield, S. A., Roze, D., Mauger, S., & Valero, M. (2013). Intergametophytic selfing and microgeographic genetic structure shape populations of the intertidal red seaweed *Chondrus crispus*. *Molecular Ecology*, *22*(12), 3242–3260.
Krueger-Hadfield, S. A., Shainker-Connelly, S. J., Crowell, R. M., & Vis, M. L. (2024). The eco-evolutionary importance of reproductive system variation in the macroalgae: Freshwater reds as a case study. *Journal of Phycology*, *60*(1), 15–25. https://doi.org/10.1111/jpy.13407
Lebret, K., Kritzberg, E. S., Figueroa, R., & Rengefors, K. (2012). Genetic diversity within and genetic differentiation between blooms of a microalgal species. *Environmental Microbiology*, *14*(9), 2395–2404.
Lemmon, P. E. (1956). A spherical densiometer for estimating forest overstory density. *Forest Science*, *2*(4), 314–320.
Lemmon, P. E. (1957). A new instrument for measuring forest overstory density. *Journal of Forestry*, *55*(9), 667–668.
Lewontin, R. C. (1964). The interaction of selection and linkage. I. General considerations; heterotic models. *Genetics*, *49*, 49–67.
Lindstrom, S. C. (1993). Inter- and intrapopulation genetic variation in species of *Porphyra* (Rhodophyta: Bangiales) from British Columbia and adjacent waters. *Journal of Applied Phycology*, *5*(1), 53–62.
Linhart, Y. B., & Grant, M. C. (1996). Evolutionary significance of local genetic differentiation in plants. *Annual Review of Ecology and Systematics*, *27*, 237–277.
Liu, F., Wu, W. Y., Wan, T., Wang, Q. F., Cheng, Y., & Li, W. (2013). Temporal variation of resource allocation between sexual and asexual structures in response to nutrient and water stress in a floating-leaved plant. *Journal of Plant Ecology*, *6*(6), 499–505.
Maggs, C. A. (1988). Intraspecific life history variability in the Florideophycidae (Rhodophyta). *Botanica Marina*, *31*, 465–490.
Neal, A. (2018). GPSCoordinates, *version 5.18*.
Olsen, K. C., Ryan, W. H., Winn, A. A., Kosman, E. T., Moscoso, J. A., Krueger-Hadfield, S. A., Burgess, S. C., Carlon, D. B., Grosberg, R. K., Kalisz, S., & Levitan, D. R. (2020). Inbreeding shapes the evolution of marine invertebrates. *Evolution*, *74*, 1–12.

Orive, M. E., Barfield, M., Fernandez, C., & Holt, R. D. (2017). Effects of clonal reproduction on evolutionary lag and evolutionary rescue. *American Naturalist*, *190*(4), 469–490.
Otto, S. P., & Marks, J. C. (1996). Mating systems and the evolutionary transition between haploidy and diploidy. *Biological Journal of the Linnean Society*, *57*(3), 197–218.
Pierre, J. S., Stoeckel, S., & Wajnberg, E. (2022). The advantage of sex: Reinserting fluctuating selection in the pluralist approach. *PLoS ONE*, *17*(8), e0272134.
R Core Team. (2022). *R: A language and environment for statistical computing*. R Foundation for Statistical Computing, Vienna, Austria.
Reynolds, L. K., Stachowicz, J. J., Hughes, A. R., Kamel, S. J., Ort, B. S., & Grosberg, R. K. (2017). Temporal stability in patterns of genetic diversity and structure of a marine foundation species (*Zostera marina*). *Heredity*, *118*(4), 404–412.
Schemske, D. W., & Lande, R. (1985). The evolution of self-fertilization and inbreeding depression in plants. II. Empirical observations. *Evolution*, *39*(1), 41–52.
Schoenrock, K. M., McHugh, T. A., & Krueger-Hadfield, S. A. (2020). Revisiting the 'bank of microscopic forms' in macroalgal-dominated ecosystems. *Journal of Phycology*, *29*, 14–29.
Shainker-Connelly, S. J., Crowell, R. M., Stoeckel, S., Vis, M. L., & Krueger-Hadfield, S. A. (2024). Population genetics of the freshwater red alga *Batrachospermum gelatinosum* (Rhodophyta) I: Frequent intragametophytic selfing in a monoicous, haploid-diploid species. *Journal of Phycology*, *60*(4), 1420–1436. https://doi.org/10.1111/jpy.13510
Sheath, R. G. (1984). The biology of freshwater red algae. *Progress in Phycological Research*, *3*, 89–159.
Sheath, R. G., & Cole, K. M. (1992). Biogeography of stream macroalgae in North America. *Journal of Phycology*, *28*(4), 448–460. https://doi.org/10.1111/j.0022-3646.1992.00448.x
Sheath, R. G., & Vis, M. L. (2015). Red algae. In *Freshwater Algae of North America* (pp. 237–264). Academic Press.
Simon, J. C., Stoeckel, S., & Tagu, D. (2010). Evolutionary and functional insights into reproductive strategies of aphids. *Comptes Rendus Biologies*, *333*(6–7), 488–496.
Stoeckel, S., Arnaud-Haond, S., & Krueger-Hadfield, S. A. (2021). The combined effect of haplodiplonty and partial clonality on genotypic and genetic diversity in a finite mutating population. *Journal of Heredity*, *112*(1), 78–91.
Stoeckel, S., & Masson, J.-P. (2014). The exact distributions of FIS under partial asexuality in small finite populations with mutation. *PLoS One*, *9*(1), e85228. https://doi.org/10.1371/journal.pone.0085228
Stoeckel, S., Becheler, R., Bocharova, E., & Barloy, D. (2024). GenAPoPop 1.0: A user-friendly software to analyse genetic diversity and structure from partially clonal and selfed autopolyploid organisms. *Molecular Ecology Resources*, *24*(1), e13886.
Storfer, A., Murphy, M., Evans, J., Goldberg, C., Robinson, S., Spear, S., Dezzani, R., Delmelle, E., Vierling, L., & Waits, L. (2007). Putting the 'landscape' in landscape genetics. *Heredity*, *98*(3), 128–142.
Tibayrenc, M., & Ayala, F. J. (2012). Reproductive clonality of pathogens: A perspective on pathogenic viruses, bacteria, fungi, and parasitic protozoa. *Proceedings of the National Academy of Sciences of the United States of America*, *109*(48), E3305–E3313. https://doi.org/10.1073/pnas.1212452109
Van Valen, L. (1965). Morphological variation and width of ecological niche. *The American Naturalist*, *99*(908), 377–390.
Vellend, M., & Geber, M. A. (2005). Connections between species diversity and genetic diversity. *Ecology Letters*, *8*(7), 767–781.
Waits, L. P., Luikart, G., & Taberlet, P. (2001). Estimating the probability of identity among genotypes in natural populations: Cautions and guidelines. *Molecular Ecology*, *10*(1), 249–256.
Waples, R. S. (1989). A generalized approach for estimating effective population size from temporal changes in allele frequency. *Genetics*, *121*(2), 379–391.
Waples, R. S. (2006). A bias correction for estimates of effective population size based on linkage disequilibrium at unlinked gene loci. *Conservation Genetics*, *7*(2), 167–184.
Weeks, S. C. (1993). The effects of recurrent clonal formation on clonal invasion patterns and sexual persistence: A Monte Carlo simulation of the frozen niche-variation model. *Source: The American Naturalist*, *141*(3), 409–427.
Whitehead, M. R., Lanfear, R., Mitchell, R. J., & Karron, J. D. (2018). Plant mating systems often vary widely among populations. *Frontiers in Ecology and Evolution*, *6*, 38.
Whitlock, M. C. (1992). Temporal fluctuations in demographic parameters and the genetic variance among populations. *Evolution*, *46*(3), 608–615.
Wickham, H. (2016). *ggplot2: Elegant graphics for data analysis*. Springer-Verlag.

SUPPORTING INFORMATION

Additional supporting information can be found online in the Supporting Information section at the end of this article.

Table S1. Water clarity and color, and stream bed composition for each date sampled per site. Site abbreviations as in Table 1.

Table S2. Oligo information for microsatellite loci used in genotyping *Batrachospermum gelatinosum* gametophytes. The assigned locus name, repeat motif, primer sequence, fluorochrome for the forward oligo, annealing temperature, and multiplex are given for all loci. Bgel_056 was always amplified in simplex PCR. Primer concentrations (nM) are given for the labeled forward (*F**), unlabeled forward (*F*), and the unlabeled reverse (R) oligos.

Table S3. Raw size ranges for each binned allele. Each locus is given along with its fluorochrome and multiplex or simplex assignment. All alleles present for each locus are listed. The minimum and maximum raw allele sizes observed are given, along with the binned allele calls. If there was only one raw size for an allele, this size is listed between the raw_min and raw_max columns.

Table S4. Null allele frequencies for each locus were determined by non-amplification after 2-3 PCR attempts. As gametophytes are haploid, non-amplification of an allele at a given locus was considered a null allele (see also Krueger-Hadfield et al., 2013). Gametophytes with a null allele at any locus were removed for subsequent analyses.

Table S5. Median per-locus linkage disequilibrium (|D'|) for each time point. At some time points, all loci were fixed and |D'| could not be calculated. In these situations, the median |D'| is indicated as not applicable ("N.A.").

Table S6. Pairwise temporal differentiation per locus at each site and time point (measured as F_{ST}). Differentiation could not be measured if the locus was fixed at both time points. In these situations, the pairwise temporal differentiation is indicated as not applicable ("N.A.").

Table S7. Freshwater red algal species observed as macroscopic gametophytic thalli at each time point sampled at AL-CRC.

Figure S1. Map of four collection sites for *Batrachospermum gelatinosum*. GPS coordinates, physiochemical measurements, and sampling dates are in Table 2.

How to cite this article: Shainker-Connelly, S., Stoeckel, S., Vis, M. L., Crowell, R. M., & Krueger-Hadfield, S. A. (2025). Seasonality and interannual stability in the population genetic structure of *Batrachospermum gelatinosum* (Rhodophyta). *Journal of Phycology*, *61*, 172–193. https://doi.org/10.1111/jpy.13539